



Grant agreement no. 243964

QWeCI

Quantifying Weather and Climate Impacts on Health in Developing Countries

M3.2.a – Prototype seamless decadal ensemble systems completed, with assessment of the predictability of precipitation and temperature over Africa in interannual and decadal time scales

Start date of project: 1st February 2010

Duration: 42 months

Lead contractor : IC3
Coordinator of milestone : IC3
Evolution of milestone

Due date : M18
Date of first draft : M19
Start of review : M20
Milestone accepted : M20

Project co-funded by the European Commission within the Seventh Framework Programme (2007-2013)		
Dissemination Level		
PU	Public	
PP	Restricted to other programme participants (including the Commission Services)	PP
RE	Restricted to a group specified by the consortium (including the Commission Services)	
CO	Confidential, only for members of the consortium (including the Commission Services)	

MILESTONE 3.2.a

Prototype seamless decadal ensemble system completed, with assessment of the predictability of precipitation and temperature over Africa in interannual and decadal time scales

This report mainly deals with the decadal prediction of the West African monsoon, Part I. The Part II deals with multi-year prediction skill of near-surface air temperature.

- PART I -

1. Introduction

The understanding and predictability of the West African monsoon (WAM) activity are fundamental for the Sudano-Sahelian countries, whose economies, mainly based on rain-fed agriculture, are vulnerable to climate variability. The analysis of rainfall variability at interannual and decadal timescales is therefore the basis for any short-term/near-term agricultural planning (Sultan et al. 2005). The *decadal prediction* aims certainly to explore the benefits of initializing coupled models, mainly prescribing the upper-ocean heat content, for getting prediction skill beyond the externally forced trend. Decadal forecasts are motivated by the evidence that current climate models can, to a certain degree, capture not only the impact of that changing atmospheric composition but also the evolution of slow natural variations of the climate system (Meehl et al. 2009; Murphy et al. 2010; Solomon et al. 2011). Besides, in the next few decades internal climate variations, particularly at regional scales, are expected to have similar amplitude compared to regional expressions of the anthropogenically forced global warming (Hawkins and Sutton 2009). The target of this study is the WAM rainfall variability. The identification of predictability sources for the WAM system at those lead times is, thus, of major relevance.

The WAM activity spans over a wide range of timescales, from intraseasonal (e.g. Sultan et al. 2003) to decadal (e.g. Folland et al. 1986), and is sensitive to both local forcing and remote influences. In this respect, Giannini et al. (2003) emphasized the action of the ocean basins surrounding the African continent on the WAM-Sahelian rainfall decadal trends, while Joly and Voldoire (2010) pointed out the role of the Gulf of Guinea sea surface temperature (SST) in the interannual modulation of the monsoonal system. The Guinean precipitation and the Sahelian rainfall account for most of the SST-forced WAM variability at interannual-to-decadal timescales. When climate models are forced with the time series of observed SSTs, they successfully reproduce the observed interannual-Guinean and decadal-Sahelian rainfall variabilities (Giannini et al. 2003, 2005; Moron et al. 2003; Lu and Delworth 2005; Tippet and Giannini 2006). Thus, the SST forcing can be considered as the dominant driver of the WAM rainfall variability. Conversely it is not the unique factor impacting rainfall in this monsoon region for at least three reasons (Fontaine et al. 2011): i) atmospheric internal variability contributes strongly to driving

the simulated precipitation variability at decadal to multi-decadal timescales (Caminade and Terray 2010); ii) land-surface vegetation processes and dust feedbacks may amplify rainfall anomalies (Biasutti et al. 2008); and iii) global warming impacts both multi-decadal SST variability and monsoonal circulation (Paeth and Hense 2004).

The challenge to correctly simulate the WAM rainfall interannual-to-decadal variability with coupled models is particularly complex because of the competence of all those physical mechanism above. A clear example of this comes from the assessment of climate-change projections for the WAM, for which no consensus has emerged regarding the impact of anticipated greenhouse gas forcing on the hydrology of the Sahel in the second half of the 21st century (Hulme et al. 2001; Druyan 2010). Caminade and Terray (2010) note the wide range of contradicting outcomes for African rainfall trends towards the end of the 21st century. And, even more drastically, Biasutti et al. (2008) find that evidence for any projection of WAM rainfall is uncertain. However, as decadal prediction bridges seasonal forecasts and climate-change projections, representing a joint problem of initial and boundary conditions, it may reveal potentially predictable components of the Guinean and Sahelian precipitation regimes.

Daunting results by Cook and Vizy (2006), nevertheless, suggest that many global climate models in the IPCC fourth assessment archive simulate flawed representations of the WAM climate. Likewise, Tippet and Giannini (2006) state that the weight given to the results of model-based studies must depend on the realism of the model used and the fidelity of its representation of physical processes. Results that hold across a variety of models are desirable given the imperfection of the models. In this report, the multi-year prediction skill of the WAM rainfall has been assessed by employing a multi-model ensemble and a perturbed-parameter ensemble that allows addressing several model-dependent conclusions as well as some problems of model uncertainty.

Focusing on the model representation for the 20th century, the studies by Joly et al. (2007) and Joly and Voltaire (2009) evaluate how state-of-the-art climate models in the third phase of the Coupled Model Intercomparison Project (CMIP3) simulate the relationship between tropical-extratropical SSTs and the WAM. They treat separately the high-frequency (i.e. interannual) and low-frequency (i.e. multi-decadal) variability. Given this partition, their results confirm that WAM precipitation is significantly connected to regional and global SST anomalies on both timescales. However, in most of the CMIP3 simulations, the interannual variability of SST is very weak in the Gulf of Guinea (the Atlantic Niño), especially along the Guinean coast. As a consequence, the influence on the monsoon rainfall over the African continent is hardly reproduced (Joly and Voltaire 2009). Joly et al. (2007) emphasizes the models' difficulty in simulating the response of the local inter-tropical convergence zone (ITCZ) to Atlantic SST anomalies. Concerning the low-frequency, only 5 among the 12 CMIP3 models capture some features of the Sahelian rainfall and its relation to a well-known inter-hemispheric SST pattern at decadal/multi-decadal timescales. All this lack of reliability in modelling results suggests that additional investigation is required to more confidently assess the relative roles of the oceanic basins in driving the WAM rainfall variability. This is particularly important for decadal prediction since multi-year forecast skill relies on the successful representation of

the SST forcings at interannual-to-decadal timescales, which are supposed to be included in the initialization from the ocean state.

2. Datasets

The study will analyze sets of 10-year climate retrospective forecasts, also known as decadal re-forecasts or hindcasts, which were produced as part of the EU-funded ENSEMBLES project (Doblas-Reyes et al. 2010). The experimental setup is at the heart of the experimental design of the decadal prediction component of the ongoing Fifth Coupled Model Intercomparison experiment (CMIP5), which will contribute to the next IPCC Assessment Report (AR5). The use of the ENSEMBLES decadal re-forecasts allows addressing several model-dependent conclusions. Two contributions addressing the problem of model uncertainty, a multi-model and a perturbed-parameter ensemble, will be used. The ENSEMBLES multi-model re-forecasts consist in 10-year long ensemble dynamical forecasts initialized once every five years over the period 1960-2005 (i.e. 1960, 1965 ...), and have three members per model and start on November 1st of each start date. The multi-model ensemble were produced by four European research centres: the European Centre of Medium-Range Weather Forecasts (ECMWF, UK), the Met Office-Hadley Centre (UKMO, UK; with the HadGEM2 climate model), IFM-GEOMAR (Germany) and CERFACS (France). The perturbed-parameter ensemble is known as Met Office Decadal Climate Prediction System (DePreSys; Smith et al. 2007, 2010) and was run using a nine-member ensemble of HadCM3 model variants. In order to assess the impact of initialization, two sets of decadal re-forecasts were run with and without initializing the contemporaneous state of the climate system; these re-forecasts will be referred to as DePreSys and NoAssim, respectively. On the other hand, the study will also analyze decadal re-forecasts performed at IC3 that are the corresponding contribution to the CMIP5 experiment. These decadal re-forecasts were performed with the climate model EC-EARTH (<http://eearth.knmi.nl/>); the use of EC-EARTH allows the project to have a suitable tool as seamless climate prediction system (Hazeleger et al. 2010).

These decadal integrations aim at exploring some indication of regional decadal predictability beyond the slow and relatively predictable warming of the planet by opening the possibility of forecasting low-frequency internal climate variability. The objective of this research is to evaluate the predictability of the low-frequency variability in the WAM rainfall.

3. Results

The period of study is 1961-2009, and the seasonal average considered July through September (JAS), which corresponds to the heart of the rainy season and when the monsoon is fully developed inland.

3.1. Rainfall indices

The forecast quality assessment of the WAM in the ENSEMBLES multi-model and perturbed-parameter decadal re-forecasts is firstly analyzed by using three different indices: i) the Guinean rainfall (hereafter GUI), precipitation anomalies averaged over 5N-10N / 10W-10E; ii) the Sahelian rainfall (hereafter SAH), precipitation anomalies averaged over 10N-18N / 15W-15E; and iii) the rainfall across a broader region including GUI and SAH (WAM index), precipitation anomalies averaged over 5N-18N / 15W-15E. Note that only land points are used in the computation.

Figure 1 shows the ensemble-mean anomaly correlation coefficient between the single forecast systems contributing to the ENSEMBLES multi-model (coloured thin lines), the multi-model ensemble-mean (MME; thick black), DePreSys (thick purple), and NoAssim (thick pink) against JAS GPCP precipitation for the GUI (top), SAH (middle) and WAM (bottom) rainfall indices. Note that a 4-year running-mean is used upon the observations and re-forecasts before the computation of the skill, and the correlation scores are shown for each 4-year average in the forecast time. No significant multi-year prediction skill is found for any of the rainfall indices, although it is clear that SAH time-series perform better with the ENSEMBLES multi-model showing systematically positive correlations along the whole forecast time (Fig. 1 middle, thick black). From the comparison between initialized (DePreSys, thick purple) and uninitialized (NoAssim, thick pink) decadal re-forecasts it is found that there is no multi-year skill in forecasting the WAM rainfall neither from the combination of greenhouse gases, solar and volcanic forcings (i.e. boundary conditions) nor from internal oceanic variability (i.e. initial conditions).

From this scenario one could argue that the prediction skill for interannual-to-decadal variability in the WAM rainfall is limited by the distinctive representation of ITCZ-related deep convection in each forecast system. This is further address in the next section. Here, Figure 2 shows the bias of each forecast system in the course of the forecast time, namely the model drift, for the GUI (top) and SAH (bottom) rainfall indices. ECMWF and CEERFACS overestimate the GUI precipitation, DePreSys and NoAssim (i.e. HadCM3) and IFM-GEOMAR underestimate it, whereas UKMO (i.e. HadGEM2) and EC-EARTH show almost no bias. Only CERFACS yields a marked, drying drift for GUI during the first four forecasting years. Concerning the SAH rainfall, UKMO, CERFACS and EC-EARTH overestimate the amount of precipitation, while ECMWF and IFM-GEOMAR underestimate it. DePreSys and NoAssim (i.e. HadCM3) show no bias. In this case, only ECMWF yields a marked, but wetting drift that gets the model closer to observations during the second half of the re-forecast. Nonetheless, it is noticeable that there is no correspondence between a better WAM representation (lesser drift) and a higher skill. Particularly apparent are for instance the cases of HadCM3 (DePreSys and NoAssim), which shows no bias but poor skill, and CERFCAS, which shows strong biases but good skill, for the SAH rainfall index (cf. Fig. 1-middle and Fig. 2-bottom).

3.2. Rainfall variability modes

The forecast quality assessment of the WAM in the ENSEMBLES multi-model and perturbed-parameter decadal re-forecasts and in the EC-EARTH ones is secondly analyzed by computing and comparing the dominant modes of WAM variability. Principal component analyses (PCA/EOF) have been carried out upon GPCC and CRU observational datasets (Figs. 3-4) and ENSEMBLES and EC-EARTH re-forecasts (Figs. 5-17). The results reveal distinct representations of the WAM in different global climate models, although common and encouraging features have emerged.

The first GPCC mode corresponds to the global-warming signature (25.5%), i.e. a zonal dipole-like anomalous pattern between eastern and western parts of the Guinean coastline (Mohino et al. 2011); the second GPCC leading mode is associated with the Sahelian mode (11.9%) and a global-scale SST pattern, including the Atlantic Multi-decadal Oscillation (AMO) SST anomalies; while, the third GPCC leading mode is tightly related to the Guinean rainfall (10.4%) and the Atlantic Niño SST anomaly (Fig. 3-top). The robustness of these results is assessed against the CRU dominant modes. The first CRU mode corresponds to the Sahelian rainfall (25%) and the second CRU mode is associated with the Guinean precipitation (10%); the associated SST patterns show the well-known inter-hemispheric pattern that includes the AMO in the Atlantic and the Atlantic Niño, respectively. There is not any dominant mode in CRU related to the global-warming (Fig. 4). The correlation between the Sahelian modes in GPCC and CRU is 0.89 in JAS annual means and 0.97 when a 4-year running-mean is applied to the time series. The correlation for the Guinean rainfall between both observational datasets is 0.77 based on annual means and 0.66 with a 4-year running-mean (Fig. 4).

The Atlantic Niño is the main driving SST pattern in all forecast systems (Figs. 5-10) except in CERFACS, for which no Guinean rainfall mode appears (Fig. 13, 18). CERFACS leading mode appears to be associated with an extratropical forcing mainly located over the Mediterranean basin, maybe related to the AMO. The signal of the AMO is pretty apparent during the first three forecast averages (1-4 to 3-6). The precipitation pattern reveals the Sahelian rainfall mode. Important land-atmosphere interactions seem to play at work driving the long-term predictability (Giannini et al. 2003, 2005). ECMWF leading mode clearly shows the dominance of the Atlantic Niño along the whole forecast time, with a right location of the ITCZ in the Gulf of Guinea that brings rain over the coastline (Fig. 5). In the UKMO, the correlation of the Guinean rainfall with the Atlantic Niño becomes stronger as the forecast time increases, although is isolately connected with it from the first forecast average, 1-4 years; the deep convection yields wetter conditions in the African continent than in ECMWF (Fig. 6). IFM-GEOMAR leading mode is linked to a SST pattern over the whole tropical band, with increasing amplitude of the Atlantic Niño along the forecast time; note that maximum loadings are over the Angola/Benguela upwelling system; the precipitation pattern is located too far off Guinean coast yielding even negative rainfall anomalies over land (Fig. 7). DePreSys (Fig. 8) and NoAssim (Fig. 9) both show a clear and isolated Atlantic Niño SST pattern during the whole re-forecast, but with larger correlation scores in the initialized hindcast (DePreSys); both leading precipitation modes strongly project onto the observed Guinean rainfall pattern. Finally, EC-EARTH leading mode is also related to anomalous

precipitation in the Gulf of Guinea except in the forecast average 5-8 in which it is the second one; however, the SST anomaly associated with the Atlantic Niño is wrongly located southwards, resulting thus in negative rainfall anomalies north of the ITCZ over the coastline (Fig. 10).

The Sahelian rainfall represents the second leading mode in all forecast systems, except in CERFACS for which it is the dominant one (Figs. 11-17). As for the Guinean rainfall, different models yield distinct areas of precipitation anomalies. However, it is worth noting how across the variety of coupled models the SST pattern associated with the Sahelian mode rightly projects onto the Atlantic signature of the observed inter-hemispheric SST signal (Fig. 3), showing in most of the cases a clear AMO-like pattern. In the ECMWF, the Sahel-related SST signature shows significant correlations off Newfoundland almost during the whole forecast time, presenting even the AMO-like teleconnection to the Mediterranean basin; although the maximum loadings appear to be in the subtropical North Atlantic (Fig. 11). In the UKMO, the prevalence of the subtropical North Atlantic SST pattern is more clear (Fig. 12). Notice again how the AMO-like signature for the first three forecast averages is pretty apparent in CERFACS (Fig. 13). IFM-GEOMAR yields a very consistent pattern reminiscent of the AMO signal along the whole forecast time, with larger scores in the middle of the re-forecast from 3-6 to 5-8 years (Fig. 14). Again DePreSys and NoAssim show similar SST signatures all along the forecast time, projecting onto an AMO-like pattern, although in this case the initialization in DePreSys gets a clear, unique signal in the northern North Atlantic in comparison with NoAssim (cf. Figs. 15-16). Finally, for EC-EARTH the AMO-like signature associated with the model Sahelian rainfall is the weakest among the forecast systems, and scarce, but noticeable (Fig. 17).

Figure 18 summarizes the above results showing the fraction of variance accounted for, respectively, the Guinean rainfall mode that is related to the Atlantic Niño (top) and the Sahelian rainfall mode associated with an AMO-like SST pattern (bottom). None of the leading precipitation EOFs in the models is significantly associated with the observed global warming, which appears to have a dominant role in GPCP (Fig. 19). Likewise, and as shown for the rainfall indices, no significant multi-year prediction skill is found for any of the rainfall EOF modes, although it is again clear that Sahelian rainfall performs better showing systematically positive correlations along the forecast time (Fig. 19).

3.3. Atlantic multi-decadal variability

Another aspect of the climate variability addressed in this study is the reproducibility of the Atlantic multi-decadal oscillation (AMO), for which a degree of predictability on annual and multi-year timescales has been found (e.g. Doblas-Reyes et al. 2011; van Oldenborgh et al. 2011). The large-scale SST pattern of the AMO is thought to be related to multi-decadal variations of the Atlantic meridional overturning circulation. The forecast quality assessment of the AMO has been performed upon the ENSEMBLES multi-model and perturbed-parameter decadal re-forecasts (García-Serrano and Doblas-Reyes 2011) as well as upon the EC-EARTH decadal re-forecasts. One of the most significant teleconnections associated with the AMO is the WAM-Sahel rainfall (e.g. van

Oldenborgh et al. 2011; Fig. 20). First results suggest that the AMO has a discernible predictive skill up to 3-6 years ahead when hindcasts are initialized from observations with respect to when they are conducted just with external forcing (un-initialized hindcasts in DePreSys system, i.e. NoAssim; Fig. 21). This conclusion appears to be consistent among the ENSEMBLES multi-model, DePreSys and EC-EARTH. In particular, the added skill by initialization in predicting the AMO during boreal summer may lead to skillful predictions of rainfall in the WAM at those lead times.

4. Summary

The climate variations in the West African monsoon (WAM) have shown to be largely affected by both internal, natural variability related to sea surface temperature and recent trends associated with global warming. The objectives of this study are i) to describe the characteristics of monsoonal rainfall at interannual and decadal timescales, and ii) to assess and improve the current forecast quality with dynamical models. The ENSEMBLES multi-model and perturbed-parameter decadal re-forecasts have been used to assess multi-year forecast skill of the Guinean and Sahelian rainfall indices and the North Atlantic multi-decadal sea surface temperature variability (AMV). Findings suggest that there is no significant skill in predicting the rainfall regimes itself, but the initialization improves the correlation for the AMV during the first half of the re-forecast. Finally, the leading WAM precipitation modes from ENSEMBLES and EC-EARTH decadal re-forecasts have been computed and compared with observational patterns. Results show that while in observations the global warming has a dominant role (GPCC), in the interannual-to-decadal forecasting systems the Atlantic Ocean is key player: the Atlantic Niño appearing to be the main, isolate forcing for the Guinean rainfall, and the AMV and its subtropical branch representing the driving force of the Sahelian precipitation. No significant skill has been found in the global climate models to re-forecast these dominant WAM modes; however, the same climate forecasting systems have shown significant ability to simulate the leading sea surface temperature phenomenon driving the precipitation. As a result of this research activity, a manuscript evaluating decadal prediction of the West African monsoon will be sent to a scientific journal in the coming weeks.

5. Future work

We plan to compute linear trends in precipitation at grid-point level, in order to argue the dominant effect of the global warming found in observations (GPCC). We also plan to use station-based in situ measurements to further check that hypothesis, although the ENSEMBLES decadal hindcasts do not show that global warming-related dominant role at any forecast time.

We also plan to assess multi-year prediction skill of the Atlantic Niño-3 SST index (ATL3; SST anomalies averaged over 20W-0E / 3S-3N, Zebiak 1993) in order to explore the reproducibility of the main SST forcing of the model WAM-EOFs in the ENSEMBLES and EC-EARTH decadal re-forecasts.

- PART II -

This second part deals with decadal prediction skill of 2-metre air temperature (hereafter T2m) over Africa in the ENSEMBLES multi-model and perturbed-parameter ensemble hindcasts. Annual values averaging November through October, according to the experimental set-up (Part I, Sec. 2), are considered. van Oldenborgh et al. (2011) point out that the ENSEMBLES multi-model ensemble (MME) shows limited skill in the global-mean temperature beyond the first year. The spatial distribution of the forecast skill has also been considered. For sea points SST is verified against ERSST v3b, land point T2m is verified against GHCN/CAMS datasets and polar regions (south of 60°S, north of 60°N) against the GISTEMP 12000km T2m dataset. Figure 22 shows the correlation skill in the total temperature forecasts (top) and the skill after subtracting the local trends in the observations and models (bottom). Note that using the model T2m field over sea instead of SST does not make a noticeable difference.

The skill of the T2m/SST forecasts including trends is shown in Fig. 22-top. The correlation coefficients have values of 0.5 to 0.8 over most of the globe, particularly over South and West Africa. These values are statistically significant at $p < 0.1$ (the threshold is $r = 0.47$ for nine independent data points using a one-sided t -test). Exceptions are SST in the North Pacific and Southern Oceans and T2m in parts of the Andes where other datasets have no data. These are all regions with low trends in the observational datasets used (not shown). The next question is how much of the skill is due to factors beyond the trend. The local trends are subtracted by regressing against CO₂ concentration from both the hindcasts and the observations, and the skill scores are then recomputed (Note that the trends are not necessarily the same in the models and the observations). The correlation coefficients are much lower without trends, see Fig. 22-bottom. There are almost as many regions with negative correlation coefficients as there are regions with positive ones. Instead, the focus is on the two target regions of the QWeCI project: South and West Africa. In the forecasting years 2-5, tropical West Africa is dominated by negative correlations while there is positive skill in northern West Africa, although it vanishes in 6-9-years forecast range. In the latter, positive correlation coefficients appear in the western area of tropical West Africa. Concerning South Africa, there appears to be consistent T2m prediction skill along the whole forecast time in tropical South Africa, to the north of Malawi. The MME shows increasing, positive correlations over southern South Africa from 2-5 to 6-9 forecasting years. Even so, Fig. 22 evidences that there is no clear skill in re-forecasting surface temperature in the ENSEMBLES multi-model beyond the global-warming trend.

This feature is further analysed by validating the initialised ENSEMBLES multi-model and perturbed-parameter (DePreSys) decadal hindcasts over different target regions, see Fig. 23. As inferred from Fig. 22, Figure 24 evidences that none of the forecast systems contributing to the multi-model yields significant skill of T2m neither for any of the forecast ranges considered (1, 2-5, 6-9) nor for any African areas, except CERFACS that shows consistent hit rate for the forecasting years 6-9. Hit rate, also known as proportion correct, is a coarse grained score that measures whether events are correctly distinguished, in this case above/below median. Also as discussed in Part I, Fig. 24 shows

that none of the single forecast systems in the ENSEMBLES multi-model has significant skill in re-forecasting the African rainfall. Figure 26 displays the proportion correct above/below median annual means for T2m and precipitation in DePreSys. It confirms that none of the initialised ENSEMBLES decadal hindcasts is able to produce skillful re-forecasts over Africa. van Oldenborgh et al. (2011) point out that surface temperature skill is mainly due to the trend. Figure 26 and 27 show the correlation between hindcasted and observed 5-year T2m and precipitation trends for the single systems in the multi-model and DePreSys, respectively. As expected, no coherence is found for re-forecasting rainfall trends (Figs. 26, 27 - bottom). The results also suggest that initialised ENSEMBLES decadal re-forecasts are not even capable of predicting local/regional trends over South and West Africa for near-surface land temperature (Figs. 26, 27 - top).

References

- Biasutti, M., I. M. Held, A. H. Sobel and A. Giannini (2008): SST forcings and Sahel rainfall variability in simulations of the twentieth and twenty-first centuries. *J. Clim.*, 21, 3471-3486.
- Caminade, C. and L. Terray (2010): Twentieth century Sahel rainfall variability as simulated by the ARPEGE AGCM, and future changes. *Clim. Dyn.*, doi 10.1007/s00382-009-0545-4.
- Cook, K. H. and E. K. Vizy (2006): Coupled model simulations of the West African monsoon system: twentieth- and twenty-first-century simulations. *J. Clim.*, 19, 3681-3703.
- Doblas-Reyes, F. J., A. Weisheimer, T. N. Palmer, J. M. Murphy, D. Smith (2010): Forecast quality assessment of the ENSEMBLES seasonal-to-decadal Stream 2 hindcasts. ECMWF Tech Memo 621, 45pp, Reading UK.
- Doblas-Reyes, F.J., M.A. Balmaseda, A. Weisheimer and T.N. Palmer (2011): Decadal climate prediction with the ECMWF coupled forecast system: Impact of ocean observations. *J. Geophys. Res. A*, doi 10.1029/2010JD015394.
- Druyan, L. M. (2010): Studies of 21st-century precipitation trends over West Africa. *Int. J. Climatol.*, doi 10.1002/joc.2180.
- Folland, C. K., T. N. Palmer and D. E. Parher (1986): Sahel rainfall and worldwide sea surface temperature. *Nature*, 320, 602-607.
- Fontaine, B., P. Roucou and P.-A. Monerie (2011): Changes in the African monsoon region at medium-term time horizon using 12 AR4 coupled models under the A1B emissions scenario. *Atmos. Sci. Lett.*, 12, 83-88.
- García-Serrano, J. and F. J. Doblas-Reyes (2011): On the assessment of near-surface global temperature and North Atlantic multi-decadal variability in the ENSEMBLES decadal hindcast. *Clim. Dyn.* (under review).
- Giannini, A., R. Saravanan and P. Chang (2003): Oceanic forcing of Sahel rainfall on interannual to interdecadal timescales. *Science*, 302, 1027-1030.
- Giannini, A., R. Saravanan and P. Chang (2005): Dynamics of the boreal summer African monsoon in the NSIPP1 atmospheric model. *Clim. Dyn.*, 25, 517-535.

Hawkins, E. and R. Sutton (2009): The potential to narrow uncertainty in regional climate predictions. *Bull. Amer. Met. Soc.*, 90, 1095-1107.

Hazeleger, W. and co-authors (2010): EC-Earth. A seamless Earth-System prediction approach in action. *Bull. Amer. Met. Soc.*, 91, 1357-1363.

Hulme et al. 2001;

Joly, M., A. Voldoire, H. Douville, P. Terray and J.-F. Royer (2007): African monsoon teleconnections with tropical SSTs: validation and evolution in a set of IPCC4 simulations. *Clim. Dyn.*, 29, 1-20.

Joly, M. and A. Voldoire (2009): Role of the Gulf of Guinea in the inter-annual variability of the West African monsoon: what do we learn from CMIP3 coupled simulations?. *Int. J. Climatol.*, doi 10.1002/joc.2026.

Lu, J. L. and T. L. Delworth (2005): Oceanic forcing of the late 20th century Sahel drought. *Geophys. Res. Lett.*, doi 10.1029/2005GL023316.

Meehl, G. A. and co-authors (2009): Decadal prediction: can it be skillful? *Bull. Amer. Meteor. Soc.*, 90, 1467-1485.

Mohino, E., S. Janicot and J. Bader (2011): Sahelian rainfall and decadal to multidecadal SST variability. *Clim. Dyn.*, doi 10.1007/s00382-010-0867-2.

Moron, V., N. Philippon and B. Fontaine (2003): Skill of Sahel rainfall variability in four atmospheric GCMs forced by prescribed SST. *Geophys. Res. Lett.*, doi 10.1029/2003GL018006.

Murphy, J. M. and co-authors (2010): Towards prediction of decadal climate variability and change. *Proced. Environ. Sci.* 1, 287-304.

Paeth, H. and A. Hense (2004): SST versus climate change signals in West African rainfall. *Clim. Change*, 65, 179-208.

Solomon, A. and co-authors (2011): Distinguishing the roles of natural and anthropogenically forced decadal climate variability. *Bull. Amer. Meteor. Soc.*, 92, 141-156.

Smith, D. M., S. Cusack, A. W. Colman, C. K. Folland, G. R. Harris and J. M. Murphy (2007): Improved surface temperature prediction for the coming decade from a global climate model. *Science*, 317, 796-799.

Smith, D. M., R. Eade, N. J. Dunstone, D. Fereday, J. M. Murphy, H. Pohlmann and A. A. Scaife (2010): Skilful multi-year predictions of Atlantic hurricane frequency. *Nat. Geosci.*, 3, 846-849.

Sultan, B., S. Janicot and A. Diedhiou (2003): The West African monsoon dynamics. Part I: documentation of intraseasonal variability. *J. Clim.*, 16, 3389-3406.

Sultan, B., C. Baron, M. Dingkuhn, B. Sarr and S. Janicot (2005): Agricultural impacts of large-scale variability of the West African monsoon. *Agric. For. Meteorol.*, 128, 93-110.

Tippet M. K. and A. Giannini (2006): Potentially predictable components of African summer rainfall in an SST-forced GCM simulation. *J. Clim.*, 19, 3133-3144.

van Oldenborgh, G. J., F. J. Doblas-Reyes, B. Wouters and W. Hazeleger (2011): Decadal prediction skill in a multi-model ensemble. *Clim. Dyn.* (under review).

Zebiak, S. E. (1993): Air-sea interaction in the equatorial Atlantic region. *J. Clim.*, 6, 1567-1586.

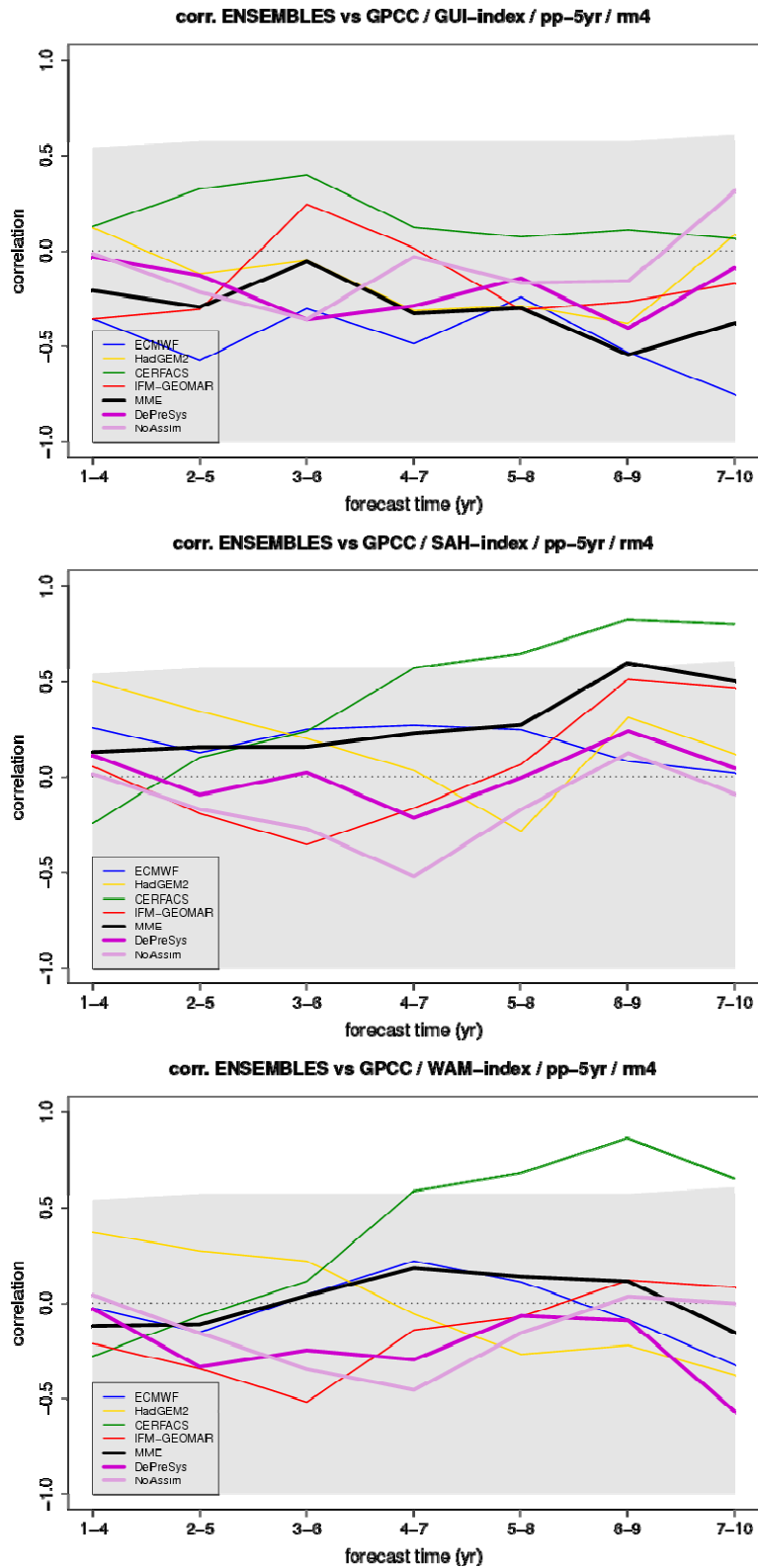


Figure 1. Ensemble-mean anomaly correlation coefficient between each single forecast system contributing to the ENSEMBLES multi-model (coloured thin lines), the multi-model ensemble-mean (MME; thick black), DePreSys (thick purple) and NoAssim (thick pink) against GPCC precipitation using July-to-September (JAS) seasonal means for: (top) the Guinean-GUI, (middle) Sahelian-SAH, and (bottom) West African monsoon-WAM rainfall indices; see text for details. All correlations have been computed with 5-year intervals between start dates. Confidence interval ($\alpha < 0.05$, one-tailed t -test) for positive, different from zero correlations are drawn in grey shading.

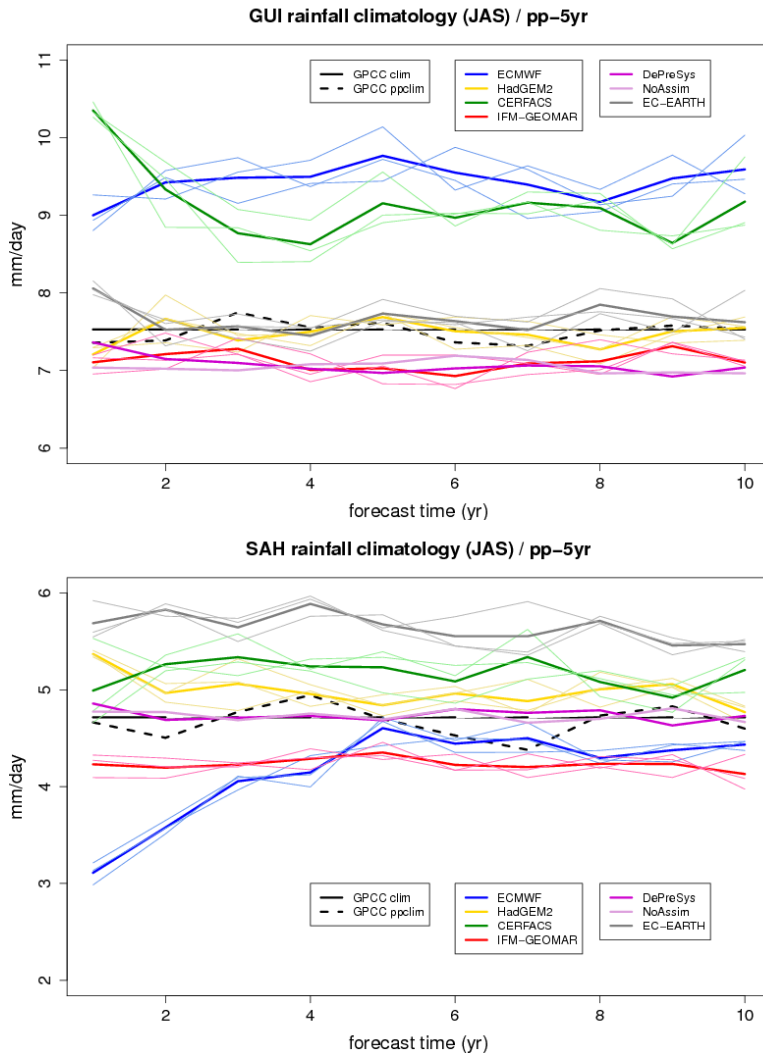
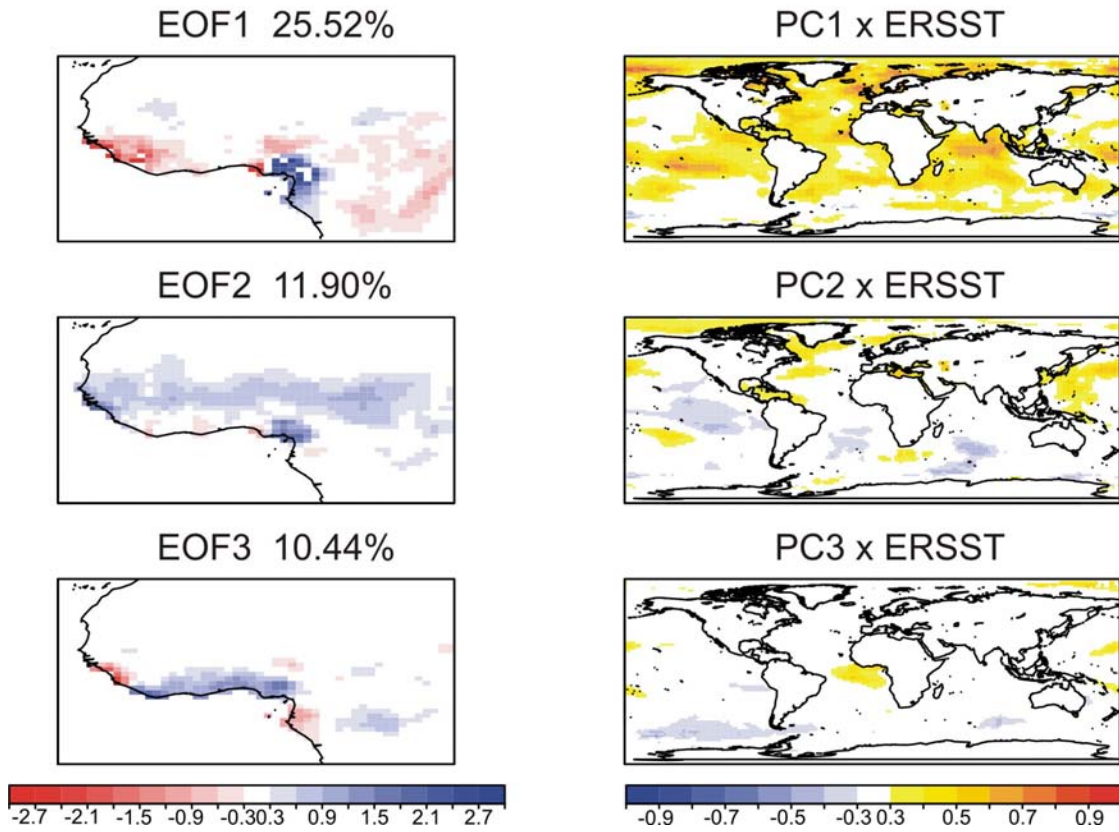


Figure 2. Evolution of the observational and model climatologies for the (top) Guinean-GUI and (bottom) Sahelian-SAH rainfall indices along the forecast time based on JAS seasonal means. GPCCC observational reference period is computed both as full-record climatology (CLIM; solid black) and as pair-pair climatology when model data is available using 5-year interval between start dates (ppCLIM; dashed black).

GPCC



CRU

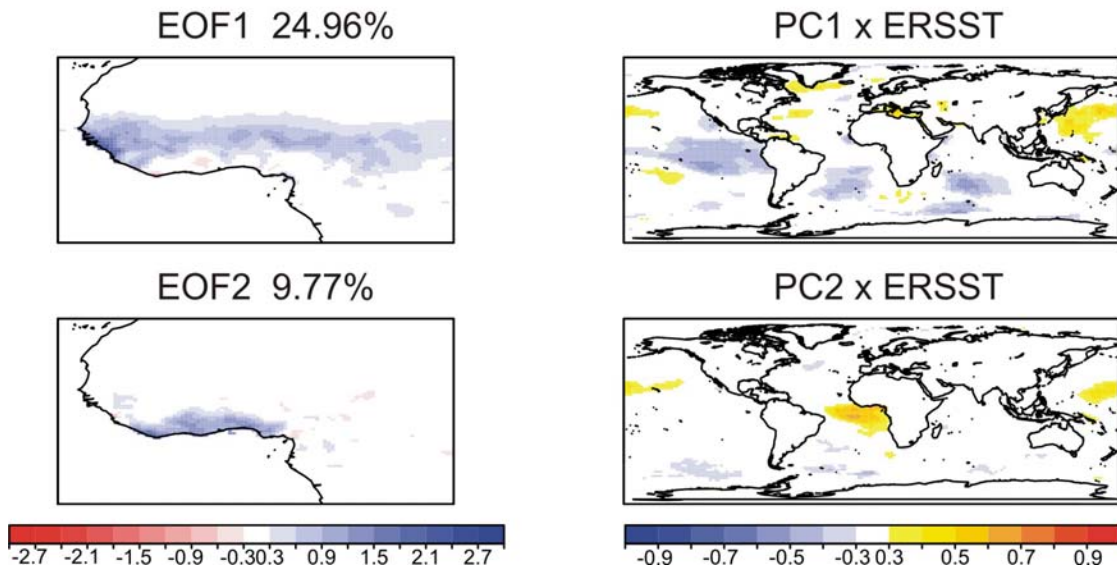


Figure 3. Empirical orthogonal functions (EOFs; mm/day) of the (top) GPCC and (bottom) CRU JAS rainfall precipitation anomalies over the WAM domain. The period of study is 1961-2009. The fraction of explained variance in each mode is indicated (in percent) together with the ordering of EOFs. The correlation maps of the corresponding standardized principal component with ERSST anomalies are shown in the right panel.

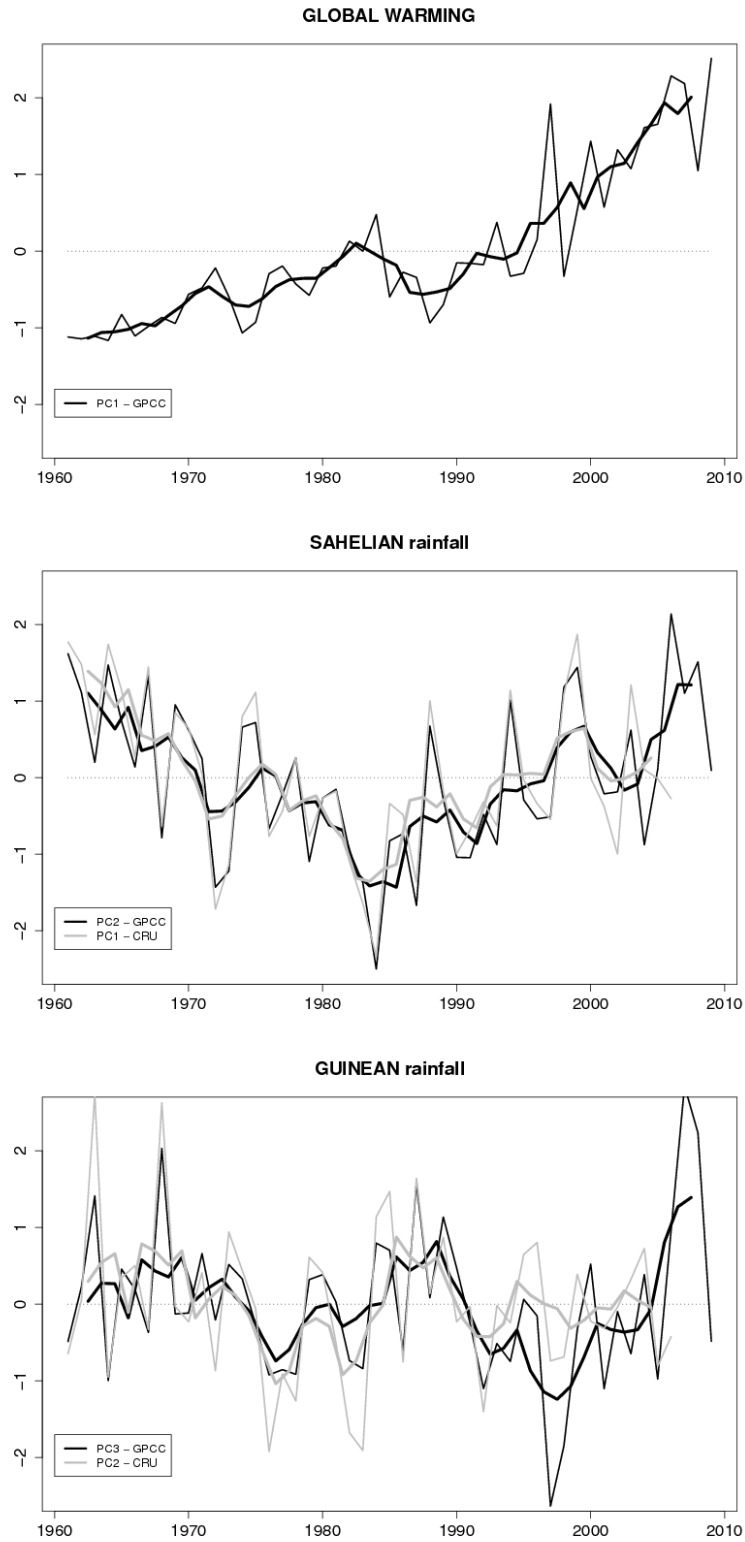


Figure 4. Standardized principal components associated with the EOFs of the GPCC (black) and CRU (grey) JAS rainfall precipitation anomalies over the WAM domain (in Fig. 3). Shown are time series based on annual means (thin lines) and a 4-year running-mean of the standardized principal components (thick lines).

ECMWF

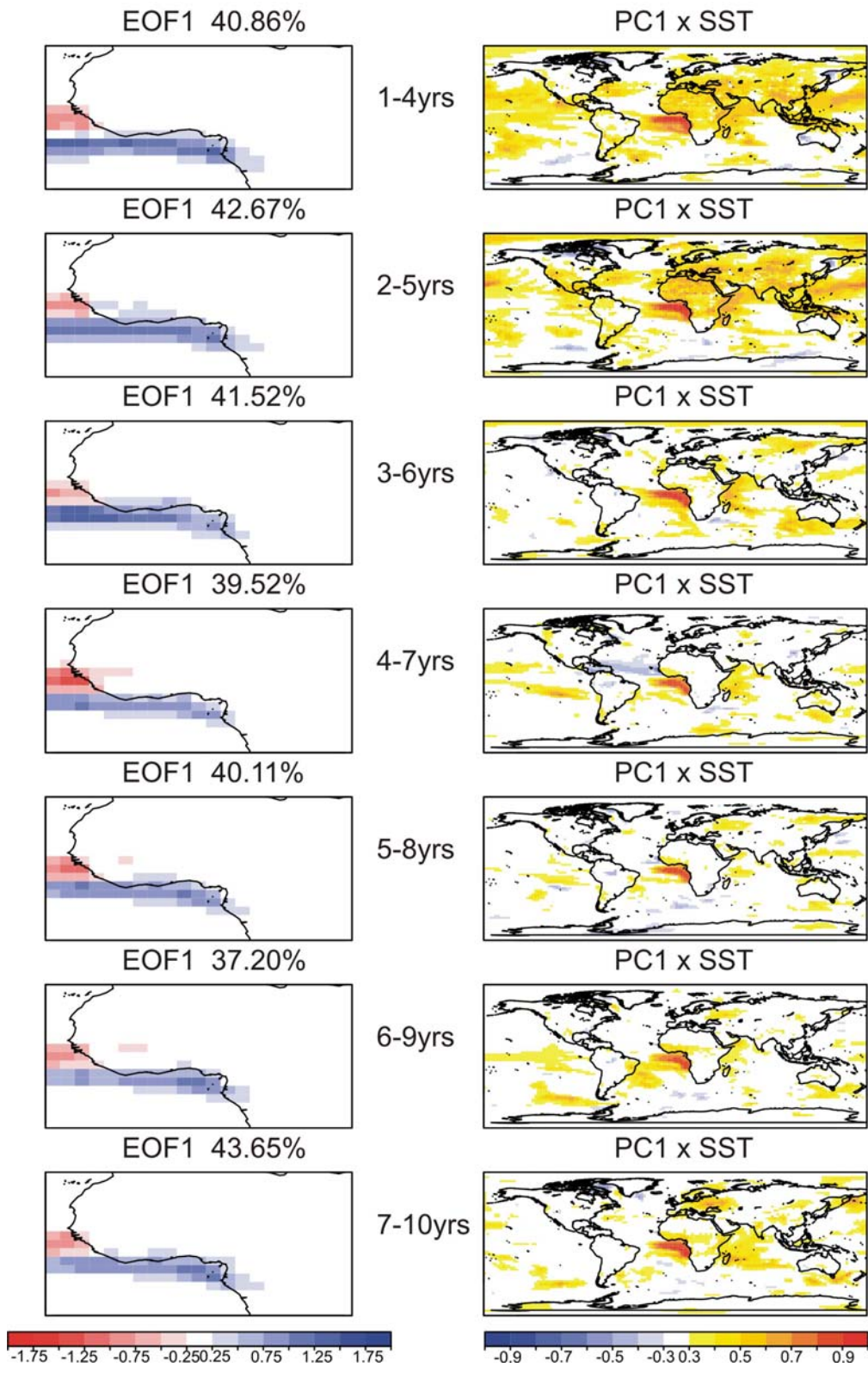


Figure 5. Guinean rainfall modes in ECMWF: empirical orthogonal functions (EOFs; mm/day) of the JAS WAM rainfall precipitation anomalies for the ECMWF climate prediction system along the forecast time every 4-year forecast average. The period of study is 1961-2009. Note that all EOFs have been computed with 5-year intervals between start dates. The fraction of explained variance in each mode is indicated in percent. The correlation maps of the corresponding standardized principal component with model SST anomalies are shown in the right panel.

UKMO

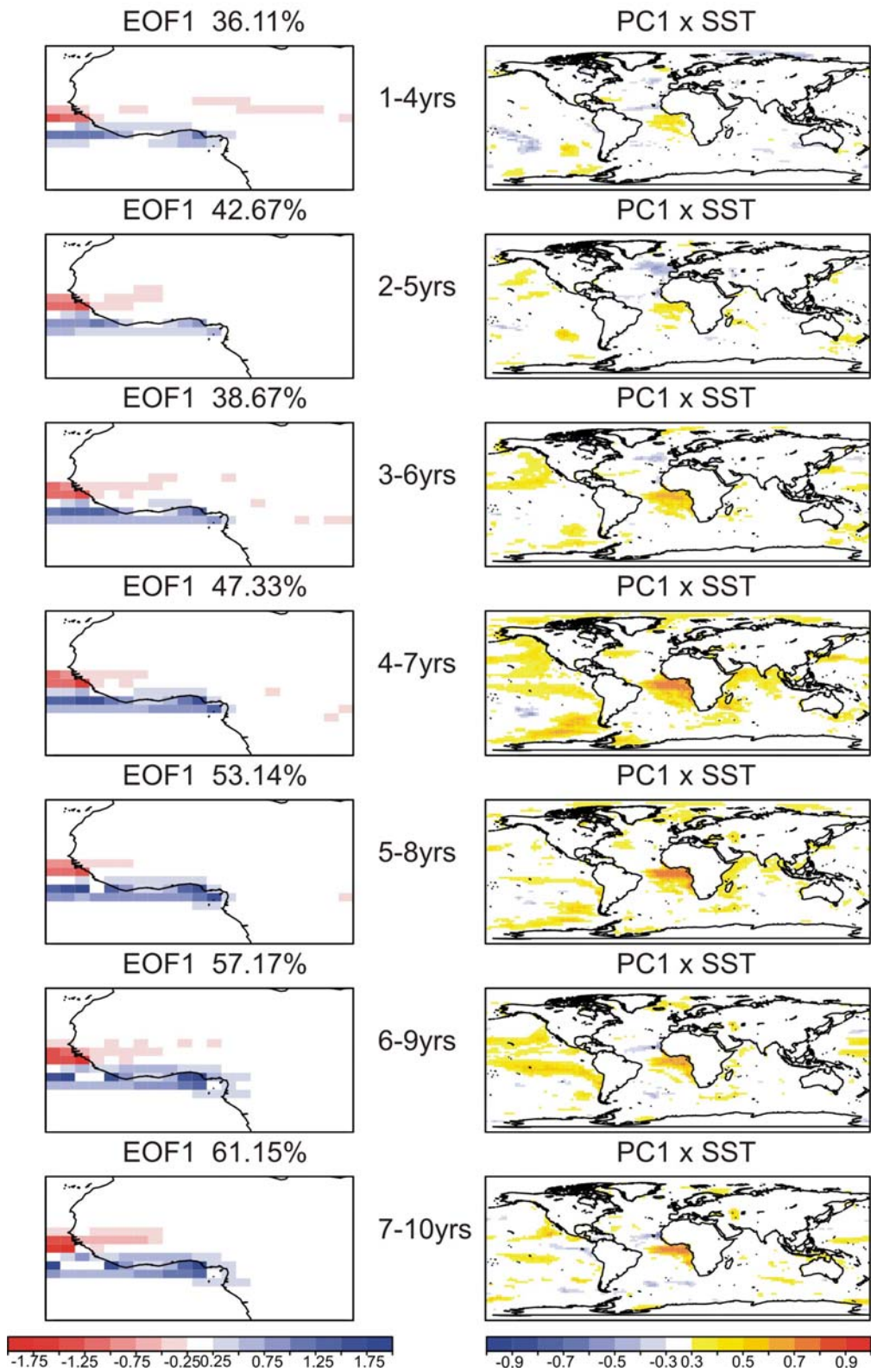


Figure 6. Same as Fig. 5 but for UKMO (HadGEM2 global climate model).

IFM-GEOMAR

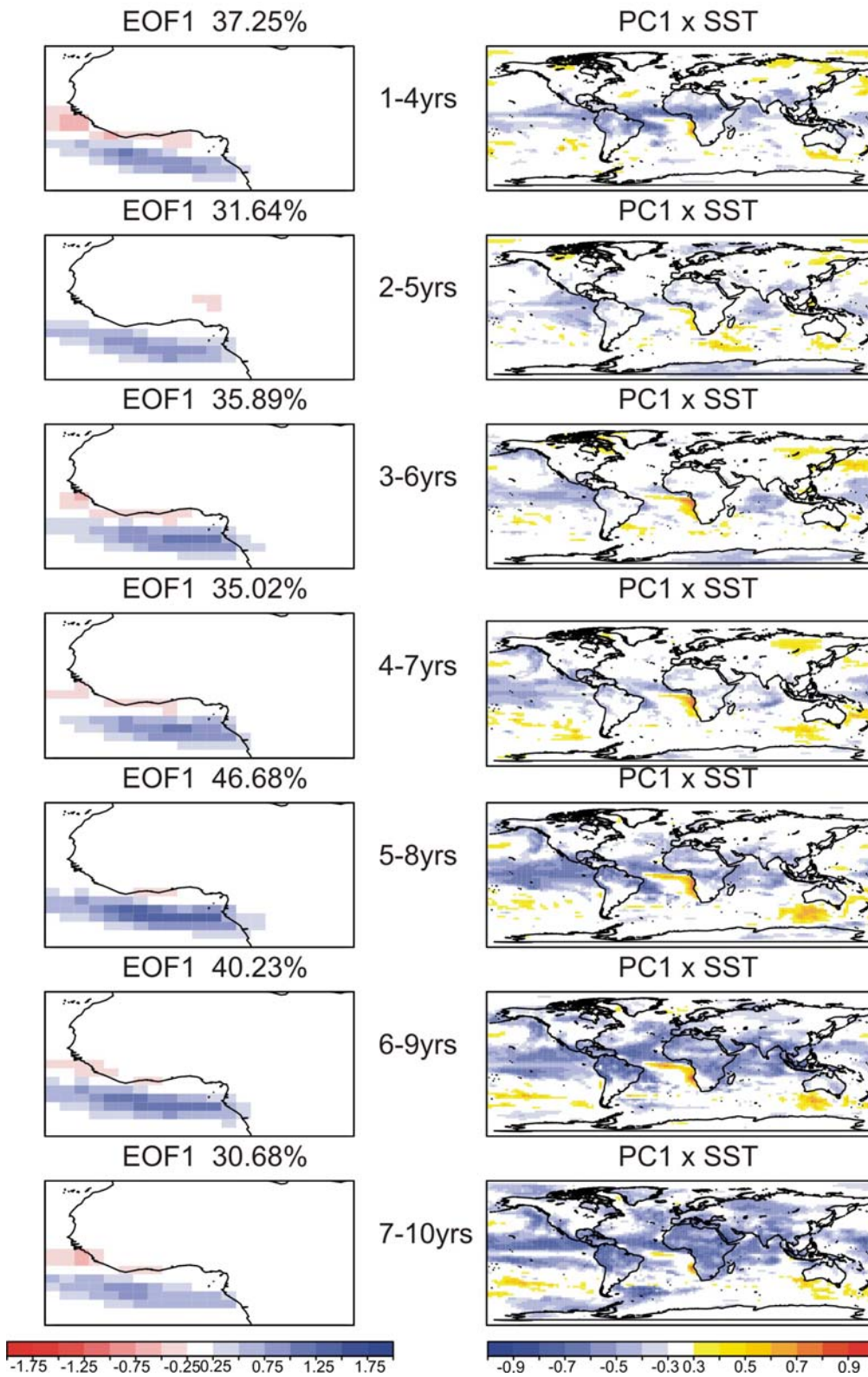


Figure 7. Same as Fig. 5 but for IFM-GEOMAR.

DePreSys

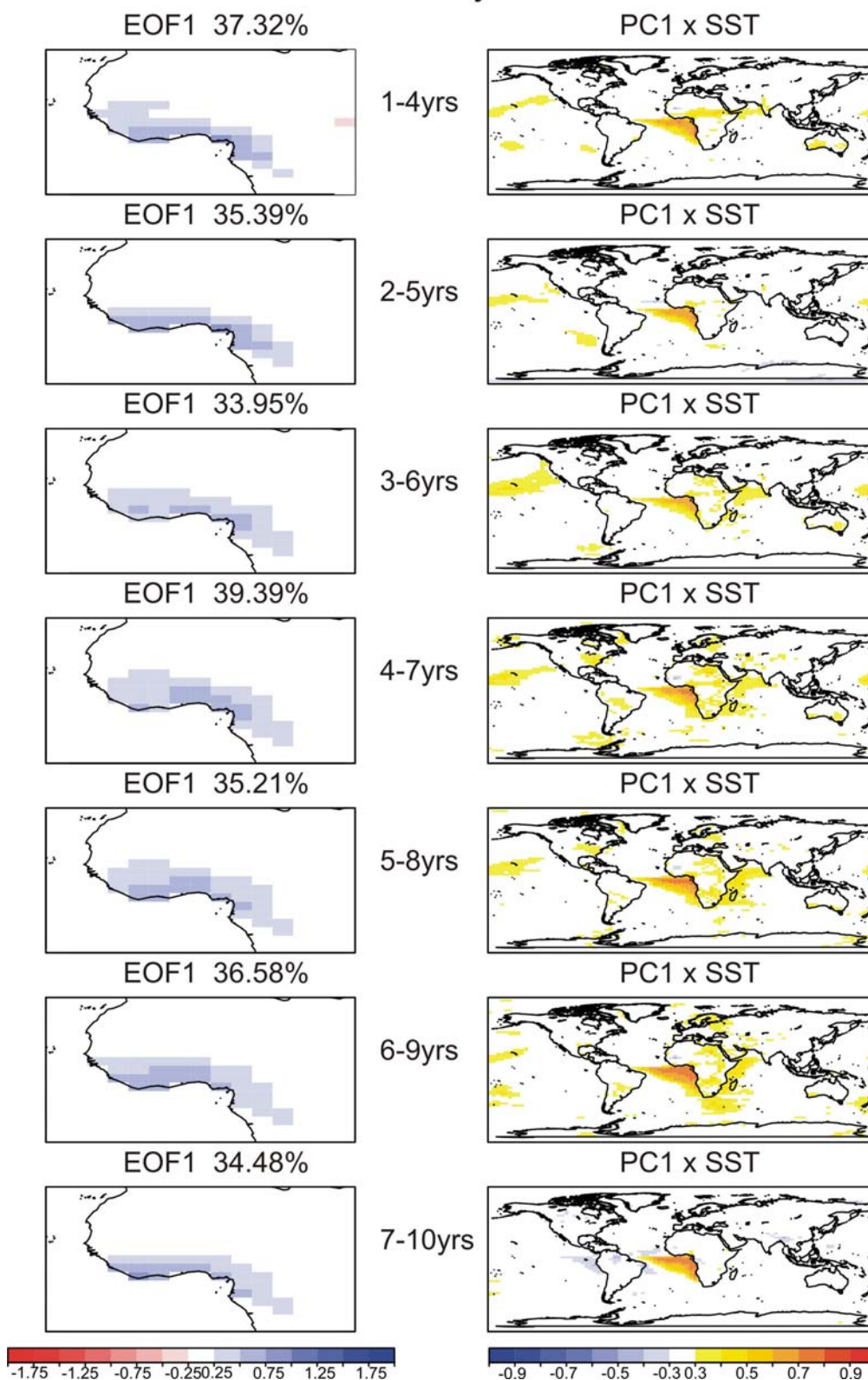


Figure 8. Same as Fig. 5 but for DePreSys.

NoAssim

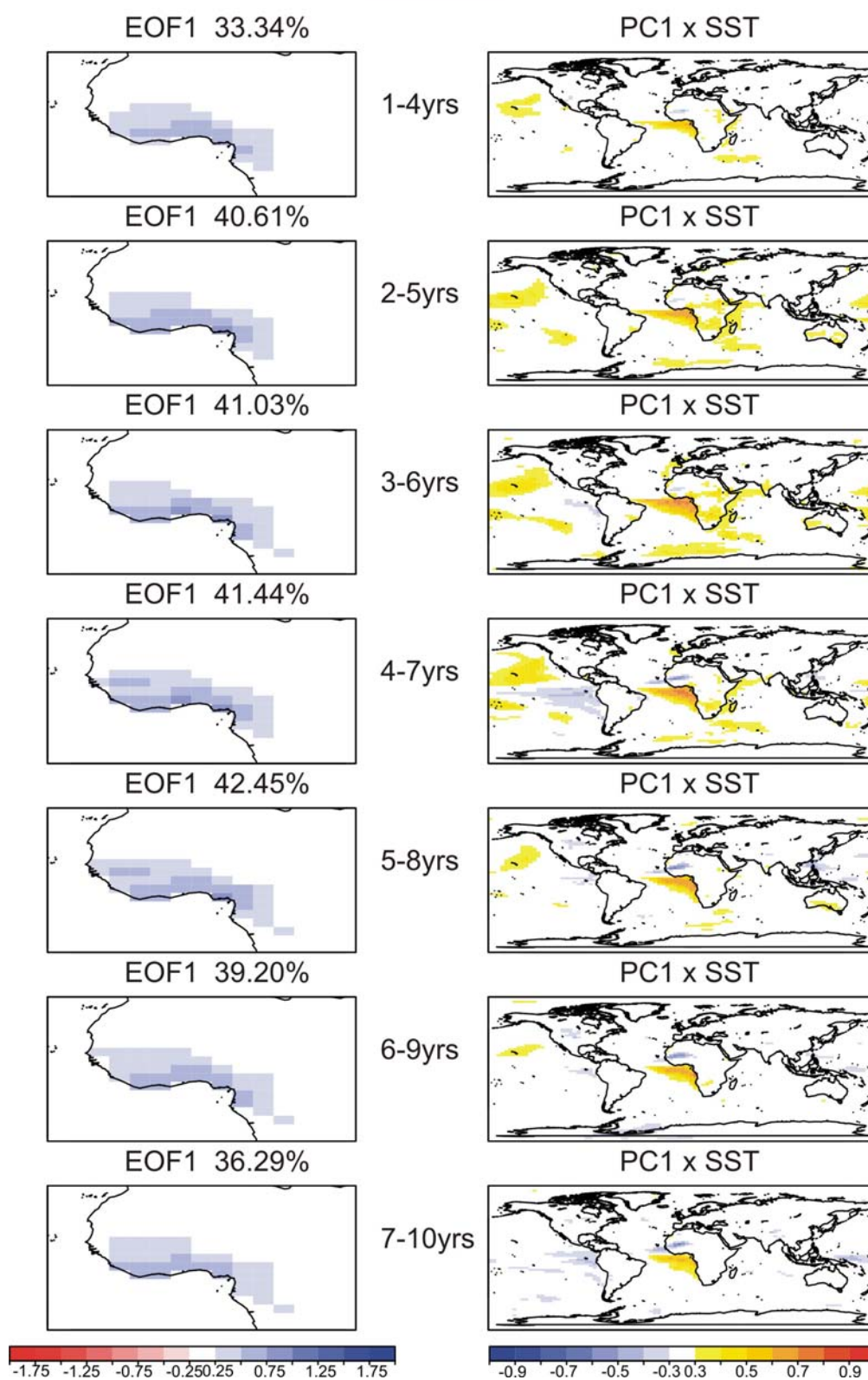


Figure 9. Same as Fig. 5 but for NoAssim.

EC-EARTH

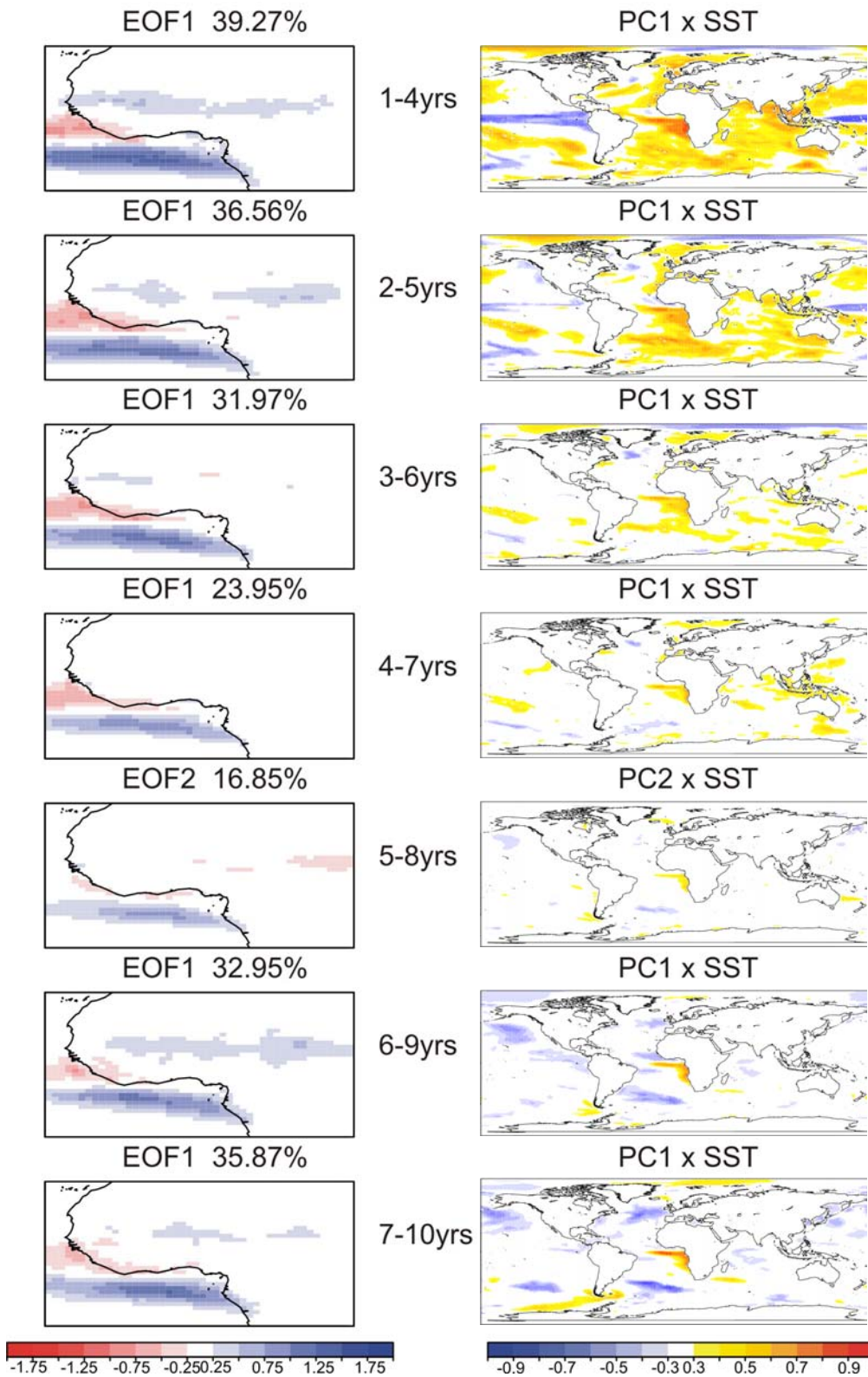


Figure 10. Same as Fig. 5 but for EC-EARTH.

ECMWF

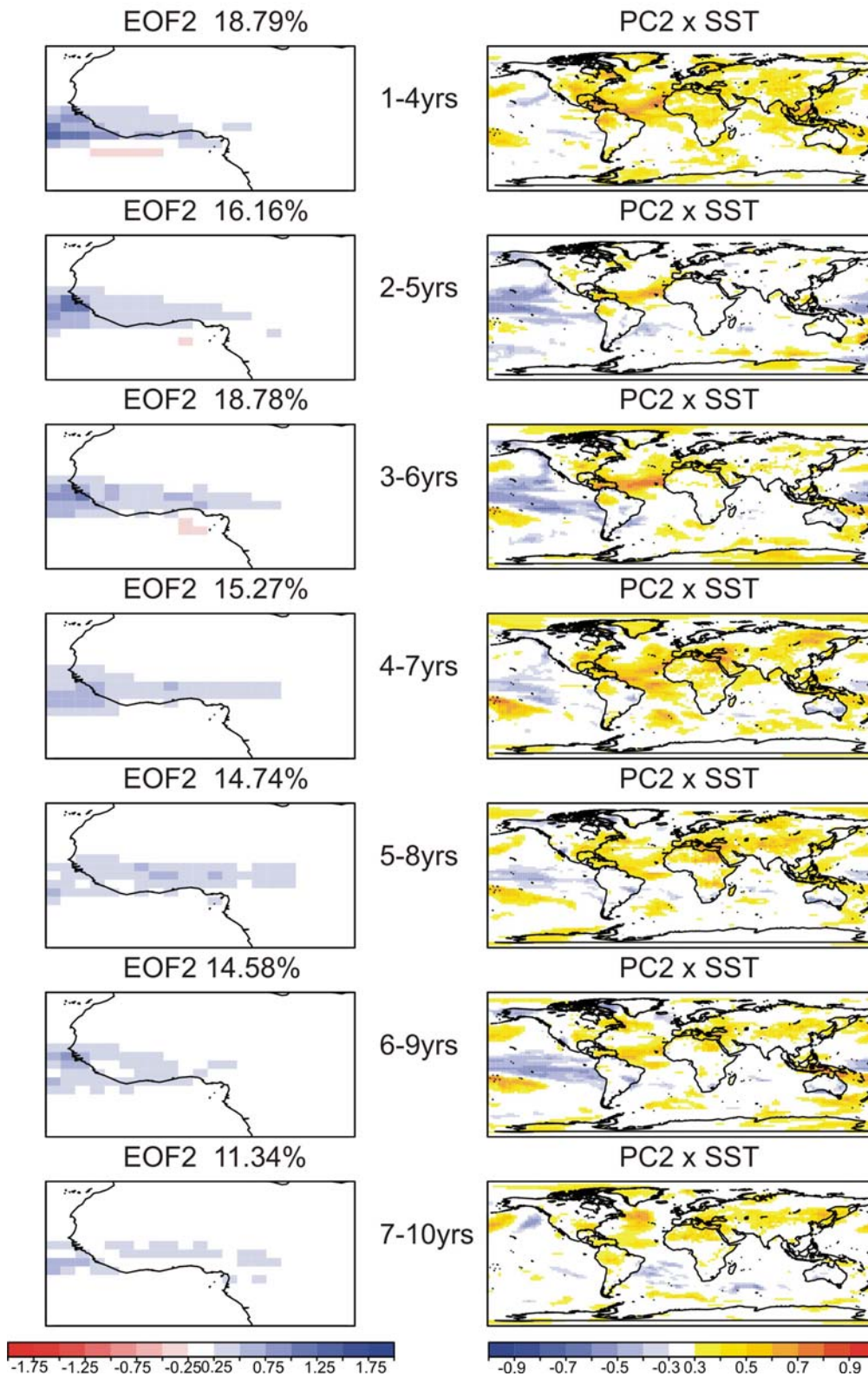


Figure 11. Sahelian rainfall modes in ECMWF: empirical orthogonal functions (EOFs; mm/day) of the JAS WAM rainfall precipitation anomalies for the ECMWF climate prediction system along the forecast time every 4-year forecast average. The period of study is 1961-2009. Note that all EOFs have been computed with 5-year intervals between start dates. The fraction of explained variance in each mode is indicated in percent. The correlation maps of the corresponding standardized principal component with model SST anomalies are shown in the right panel.

UKMO

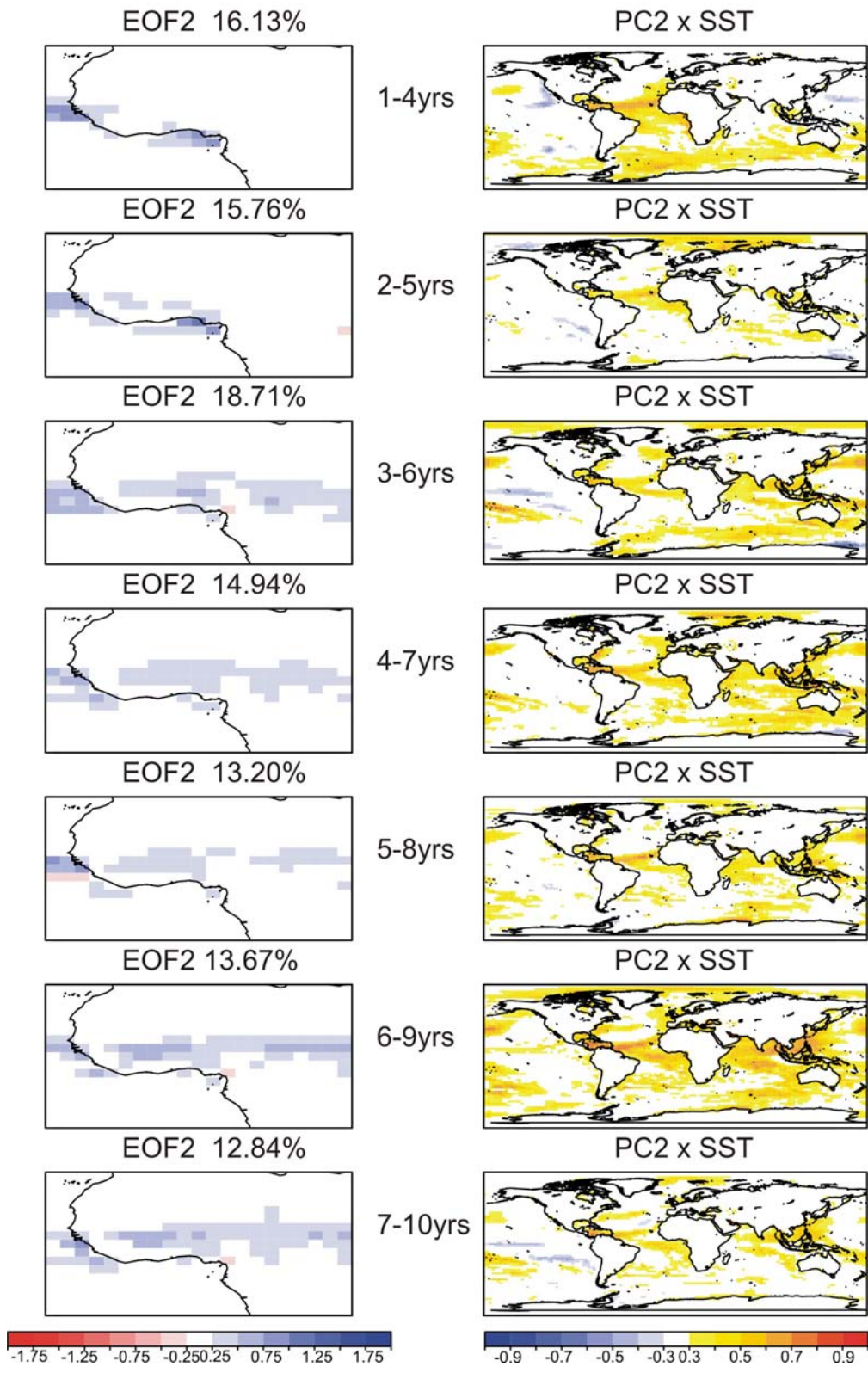


Figure 12. Same as Fig. 11 but for UKMO (HadGEM2 global climate model).

CERFACS

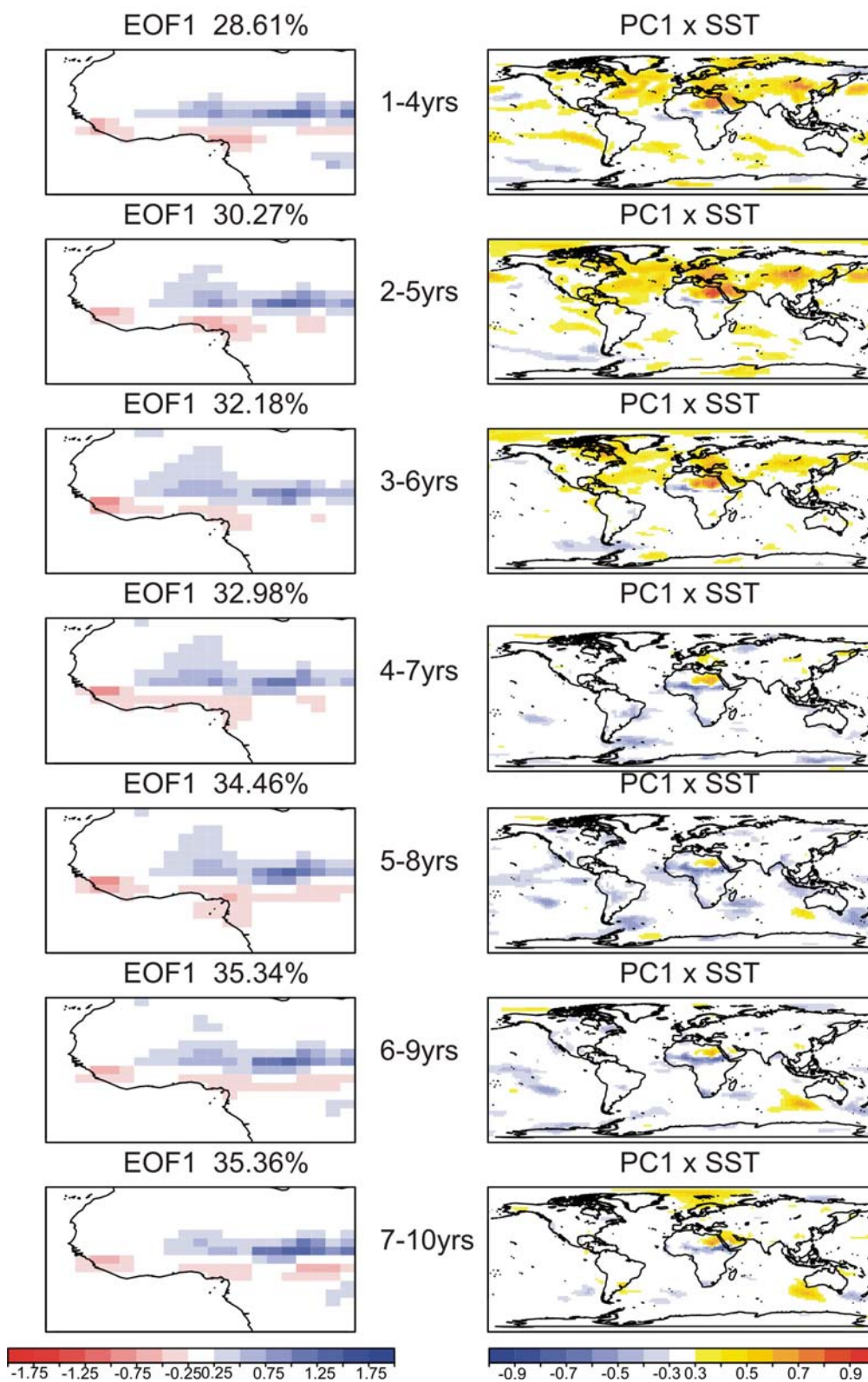


Figure 13. Same as Fig. 11 but for CERFACS.

IFM-GEOMAR

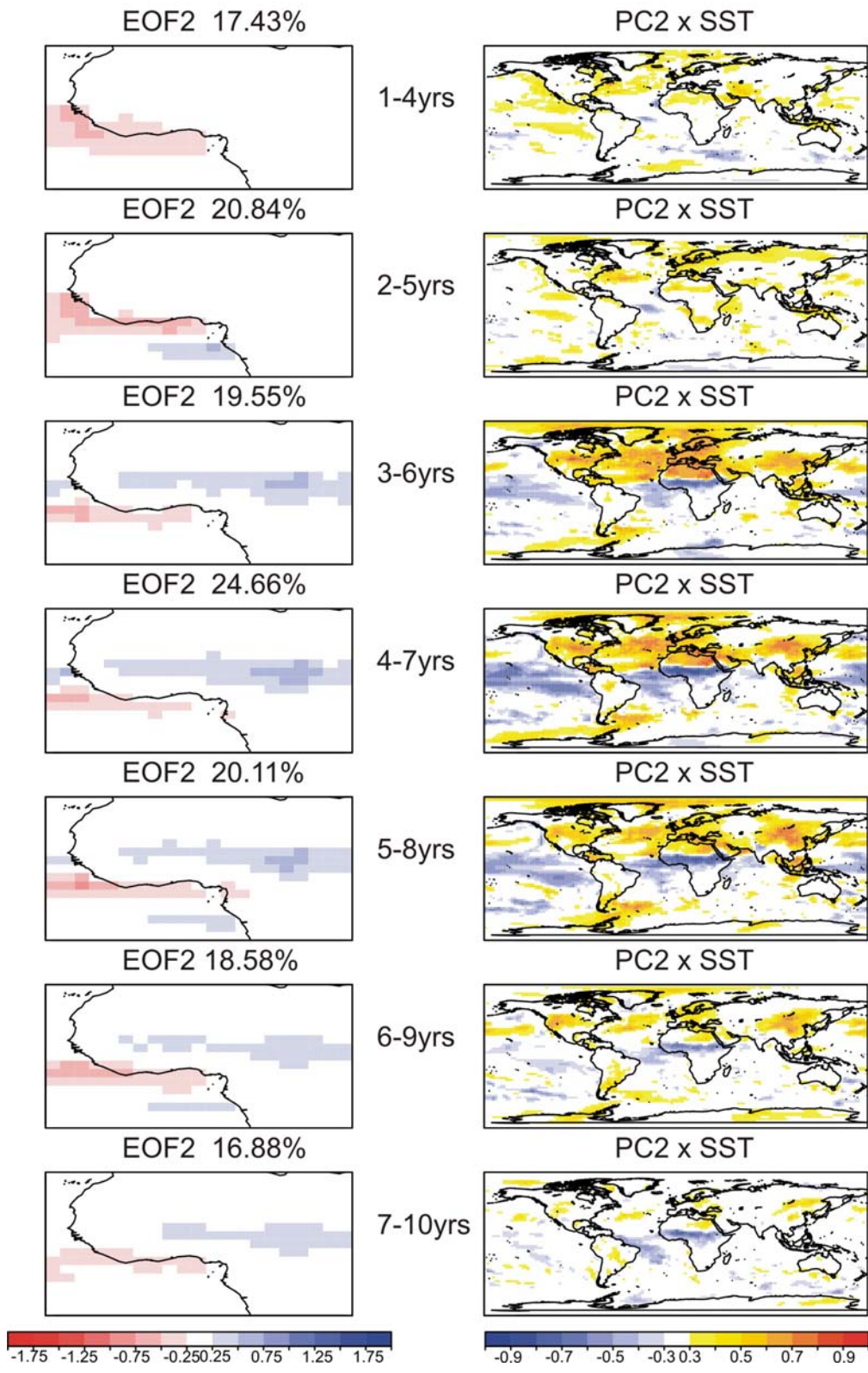


Figure 14. Same as Fig. 11 but for IFM-GEOMAR.

DePreSys

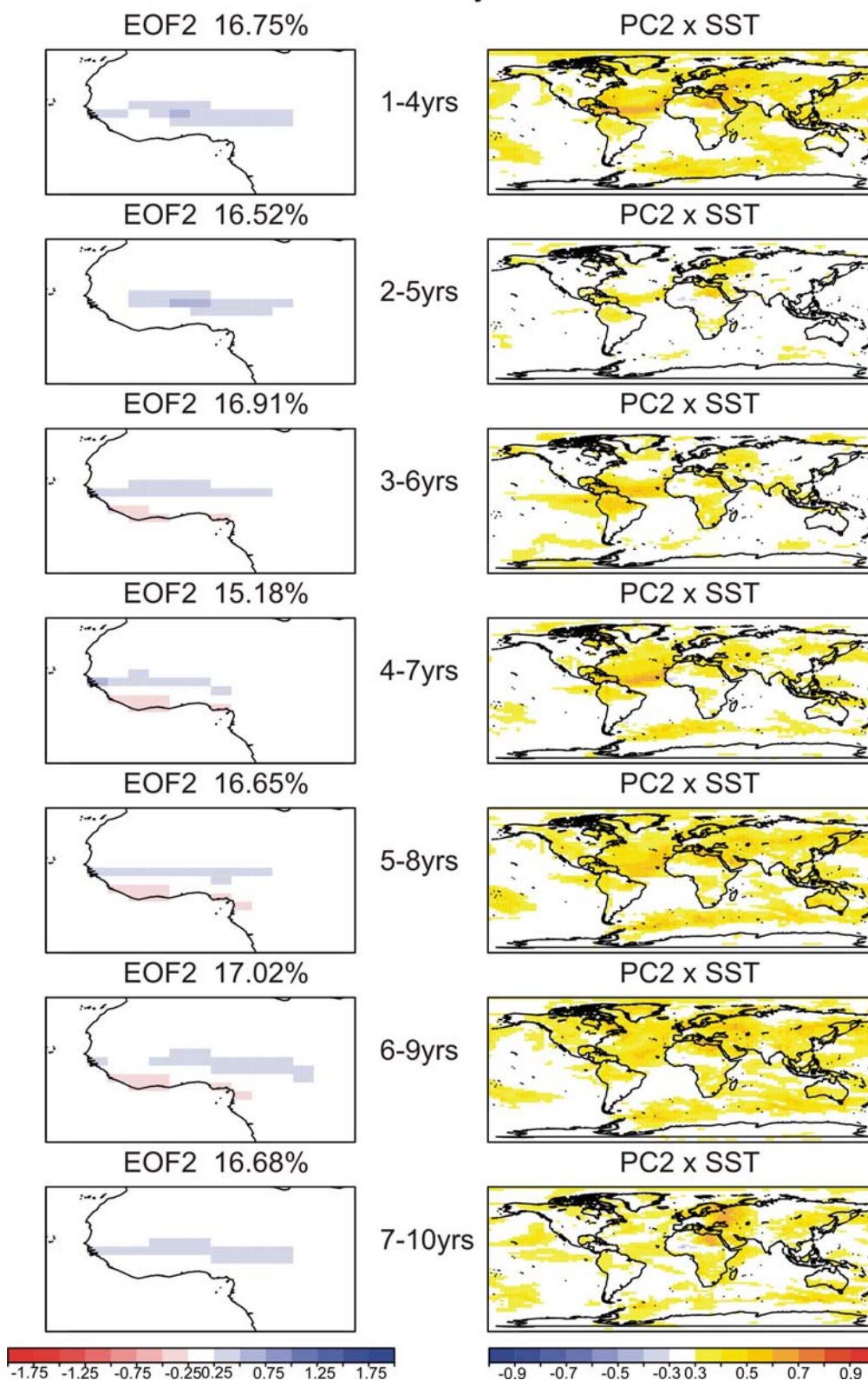


Figure 15. Same as Fig. 11 but for DePreSys.

NoAssim

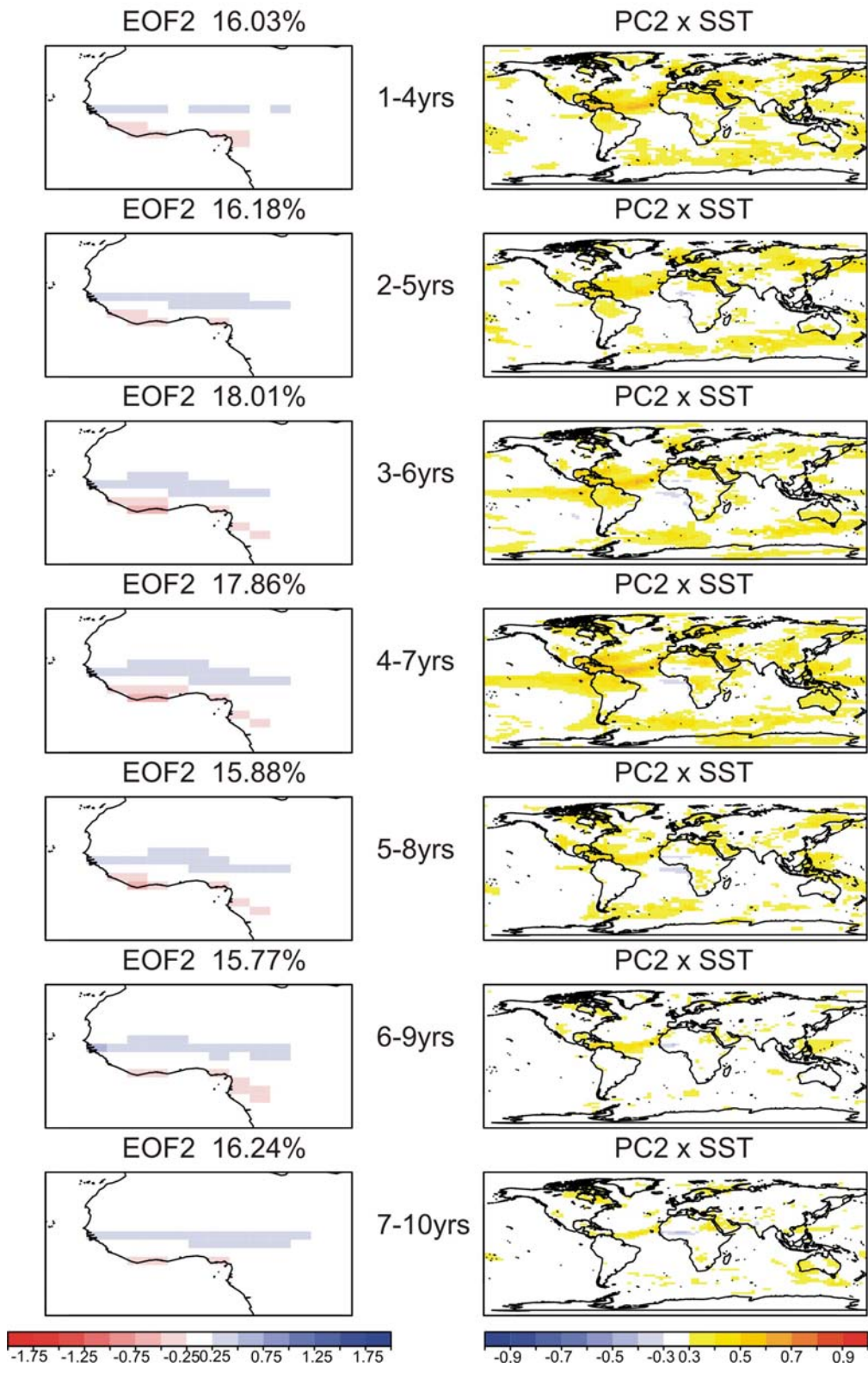


Figure 16. Same as Fig. 11 but for NoAssim.

EC-EARTH

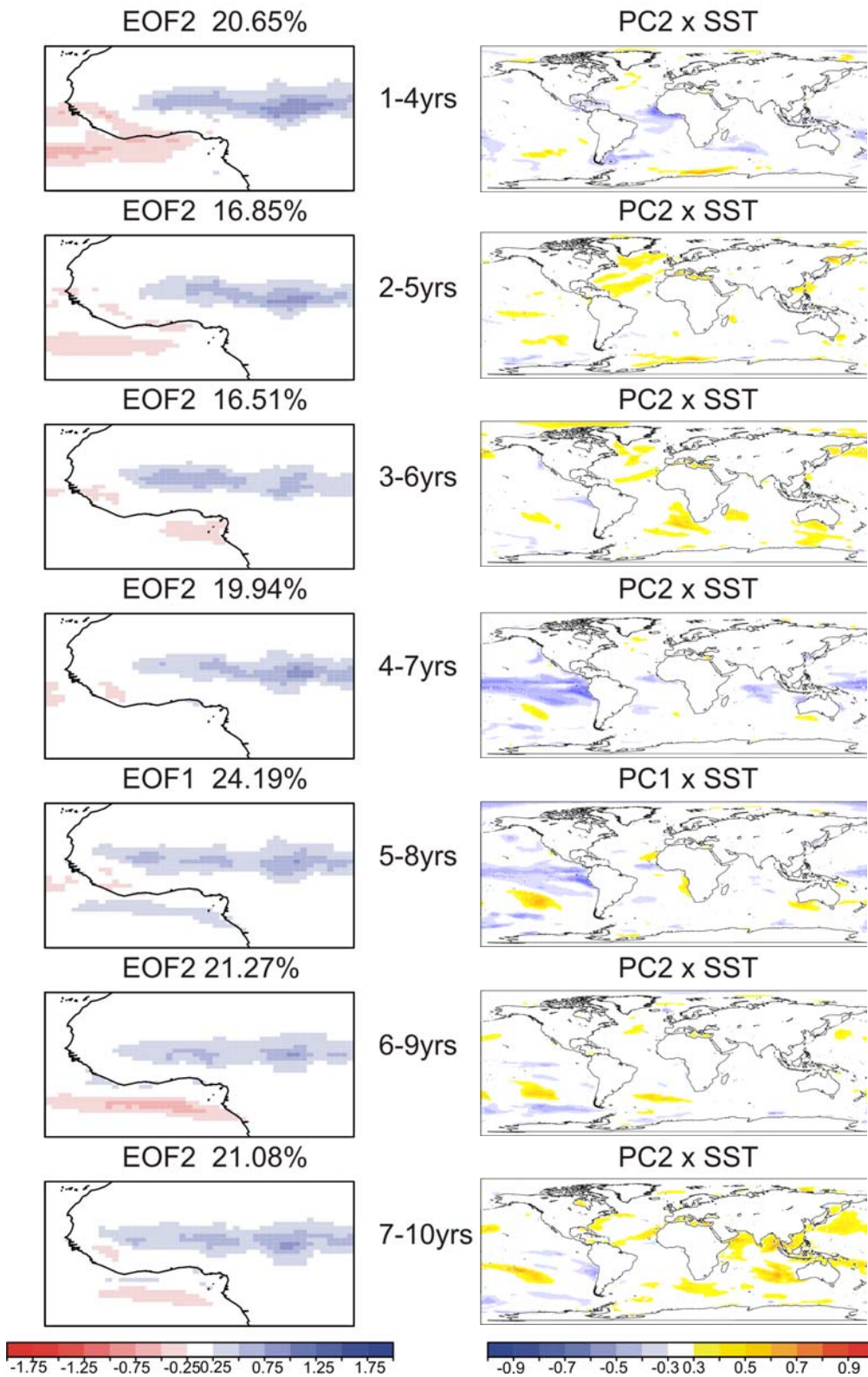


Figure 17. Same as Fig. 11 but for EC-EARTH.

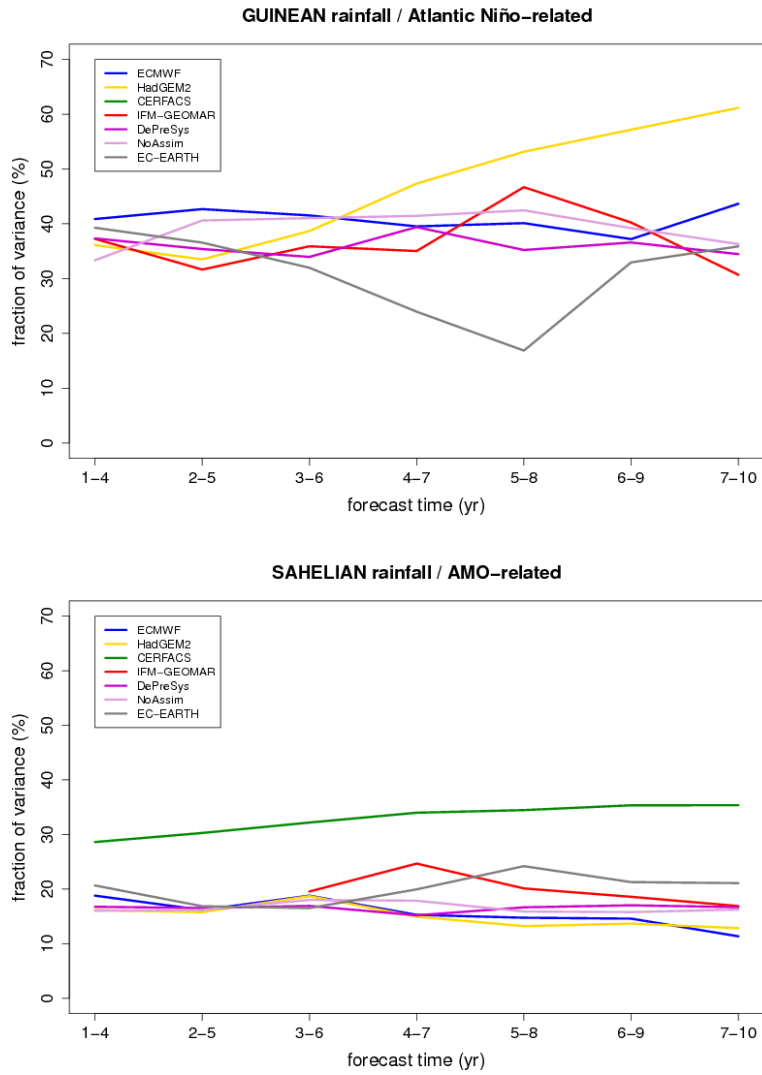


Figure 18. Fraction of explained variance in the ENSEMBLES multi-model and perturbed-parameter as well as EC-EARTH climate prediction systems, along the forecast time every 4-year forecast average, for the (top) Guinean and (bottom) Sahelian rainfall modes. The period of study is 1961-2009. Note that all EOFs have been computed with 5-year intervals between start dates.

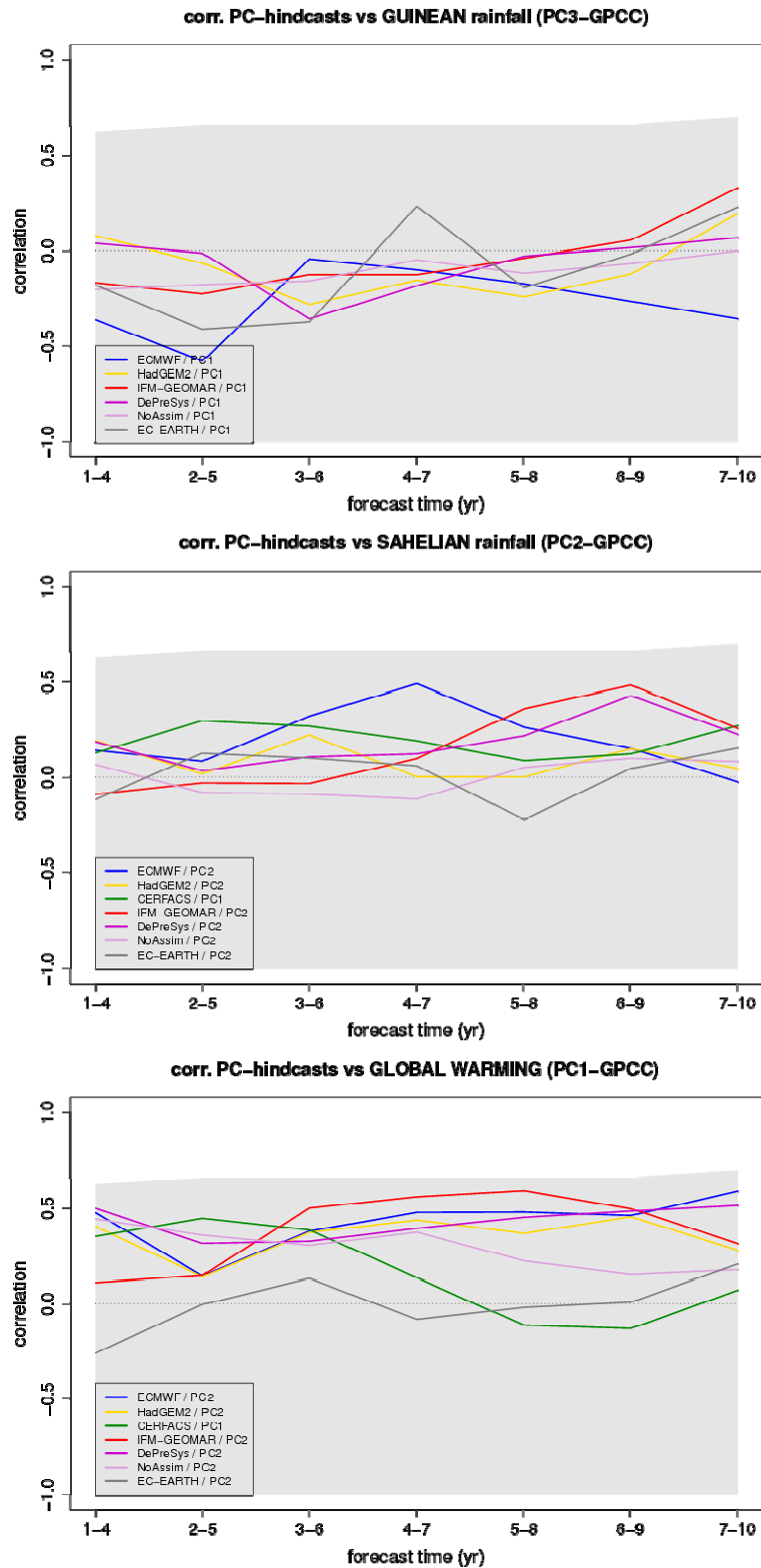


Figure 19. Anomaly correlation coefficient between the leading JAS WAM rainfall standardized principal components of each single forecast system contributing to the ENSEMBLES multi-model, DePreSys (purple), NoAssim (pink), and EC-EARTH (grey) against JAS GPCC dominant modes: the (top) Guinean and (middle) Sahelian rainfall modes, and (bottom) the pattern associated with the global warming. All EOFs have been computed with 5-year intervals between start dates. Confidence interval ($\alpha < 0.05$, one-tailed t -test) for positive, different from zero correlations are drawn in grey shading.

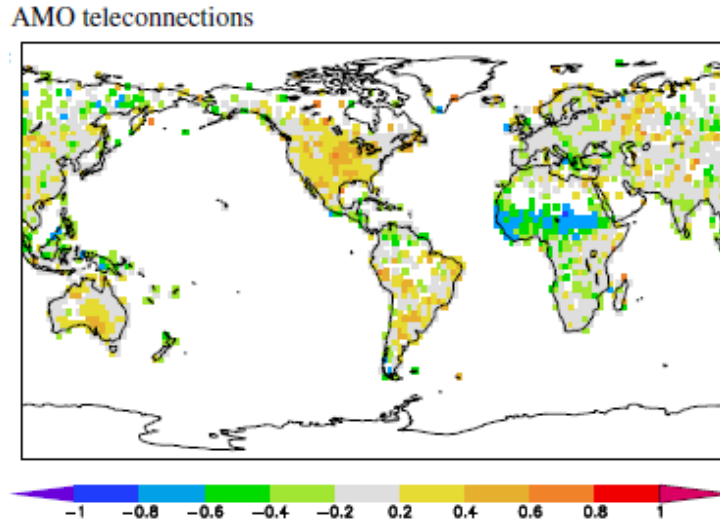


Figure 20. Correlation map of GPCP precipitation onto the AMO index over 1901-2007, demanding at least one observation per 2.5° grid box; white areas do not have enough observations to compute a correlation coefficient. [Modified from van Oldenborgh et al. 2011]

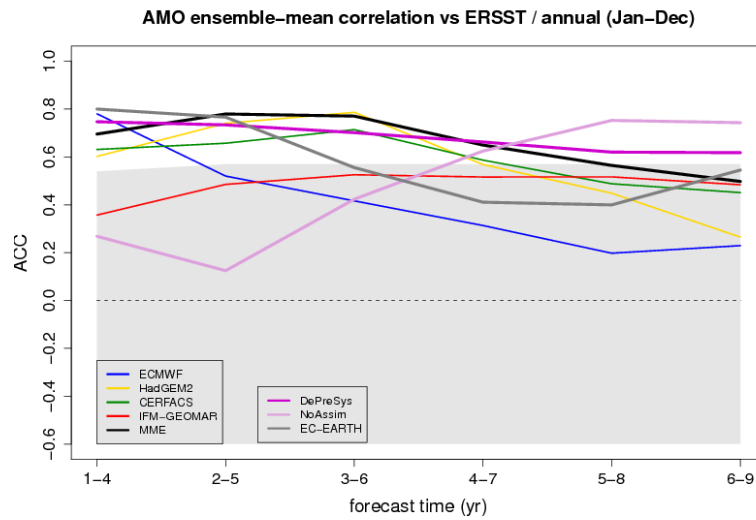


Figure 21. Ensemble-mean anomaly correlation coefficient (ACC) for the AMO index between each single forecast system contributing to the ENSEMBLES multi-model (coloured lines), the multi-model ensemble-mean (MME; thick black), DePreSys (thick purple), NoAssim (thick pink), and EC-EARTH (thick grey) against ERSST. All correlations have been computed with 5-year intervals between start dates. Annual means (January through December) have been considered with a 4-year running-mean in the forecast time. Confidence interval ($\alpha < 0.05$, one-tailed t -test) for positive, different from zero correlations are drawn in grey shading.

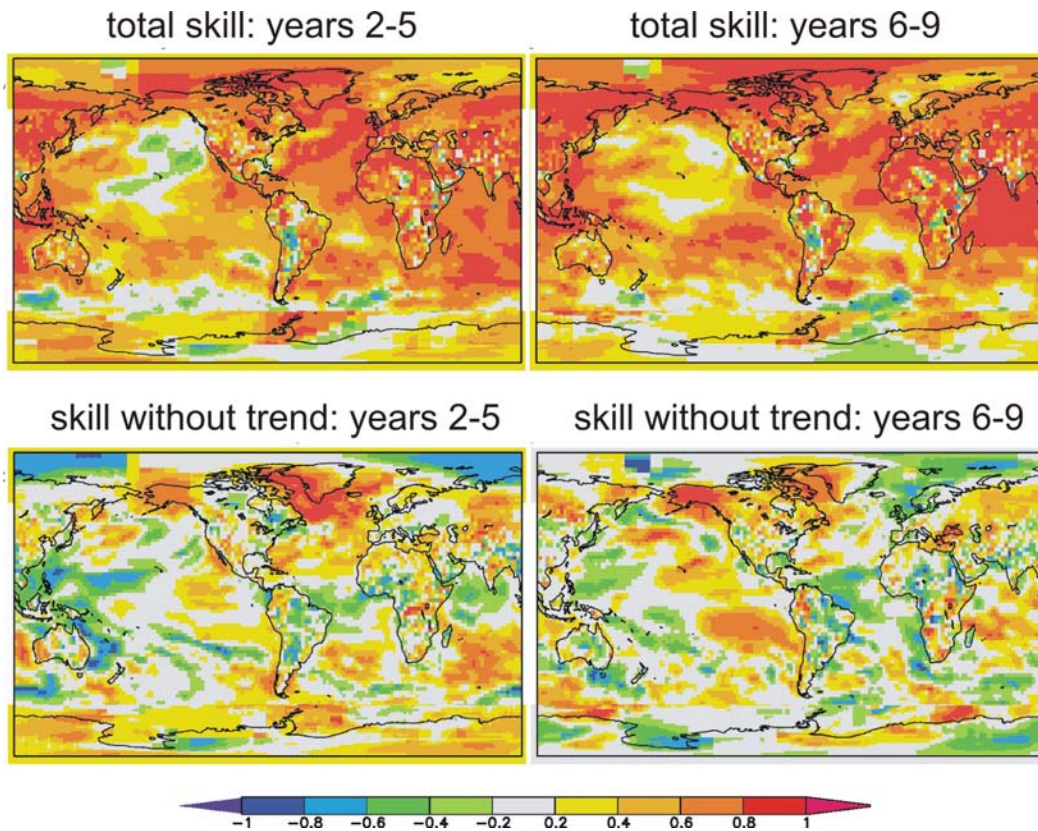


Figure 22. Correlation skill of T2m/SST hindcasts for forecasting years 2-5 (left) and 6-9 (right) including the trend (top) and the skill that is left after subtracting the local trends (regression on the CO₂ concentration) of both model and observations (bottom). Correlations are significant at p<10% for r>0.47. SST: ERSST v3b from NCDC; T2m: GHCN/CAMS from NCEP; polar regions: GISTEMP (1200km decorrelation).

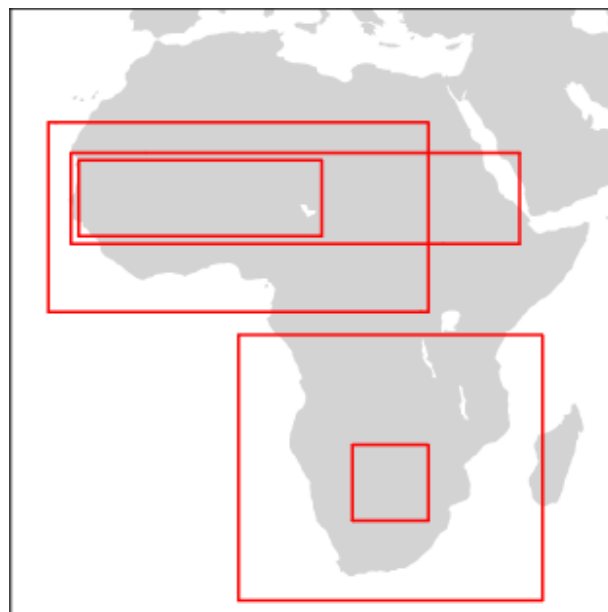


Figure 23. Regions under study of ENSEMBLES decadal hindcast validation over Africa.

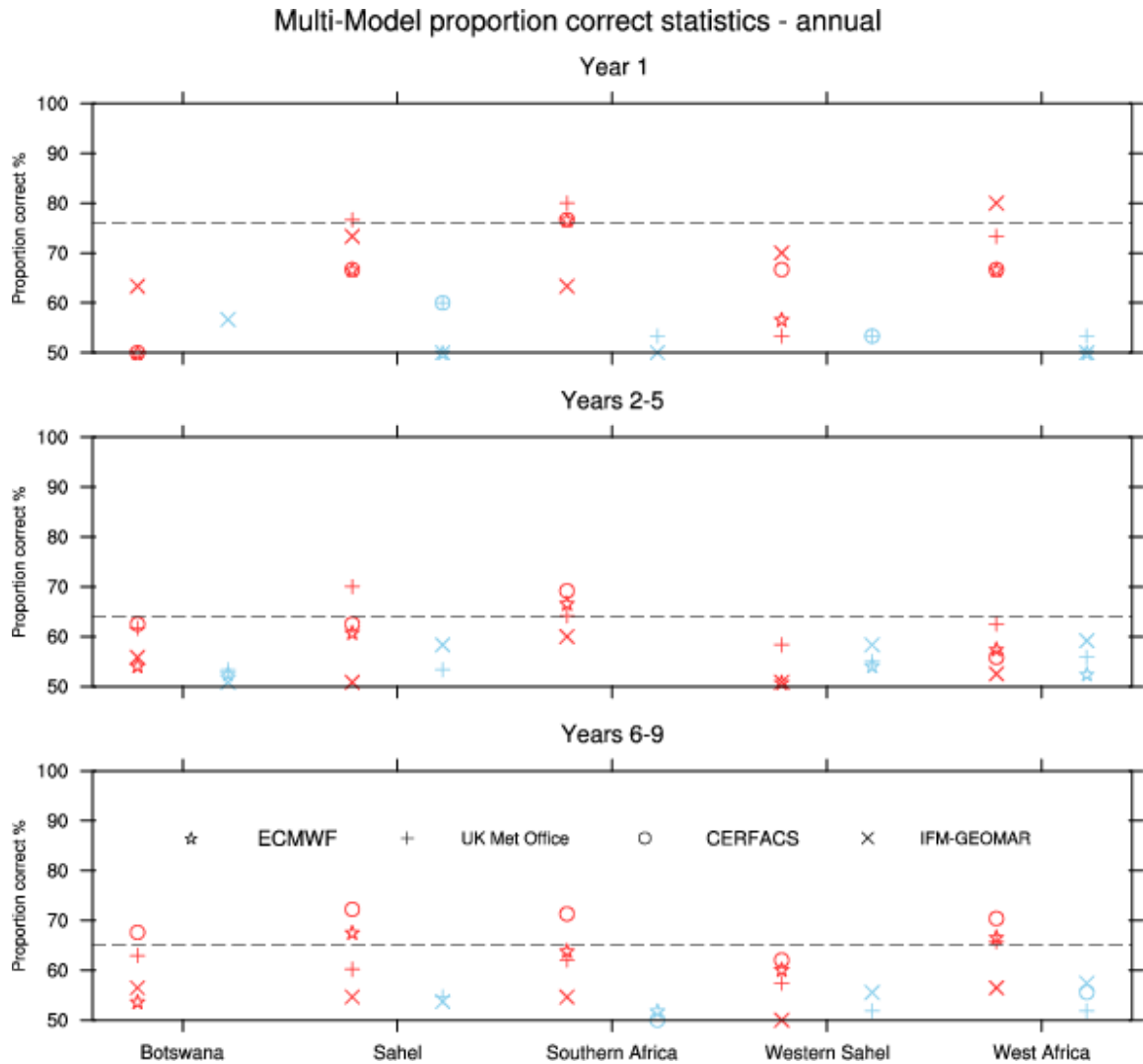


Figure 24. Proportion correct above/below median annual averages for the ENSEMBLES decadal multi-model experiment, for the regions in Fig. 23 and forecasting years 1 (top), 2-5 (middle) and 6-9 (bottom). Red corresponds to 2-metre temperature (T2m); blue, precipitation. Note that the ocean is masked in all calculations. Dashed line indicates 95% significance level. Note Y axis starts at 50%, any results below this level are not shown.

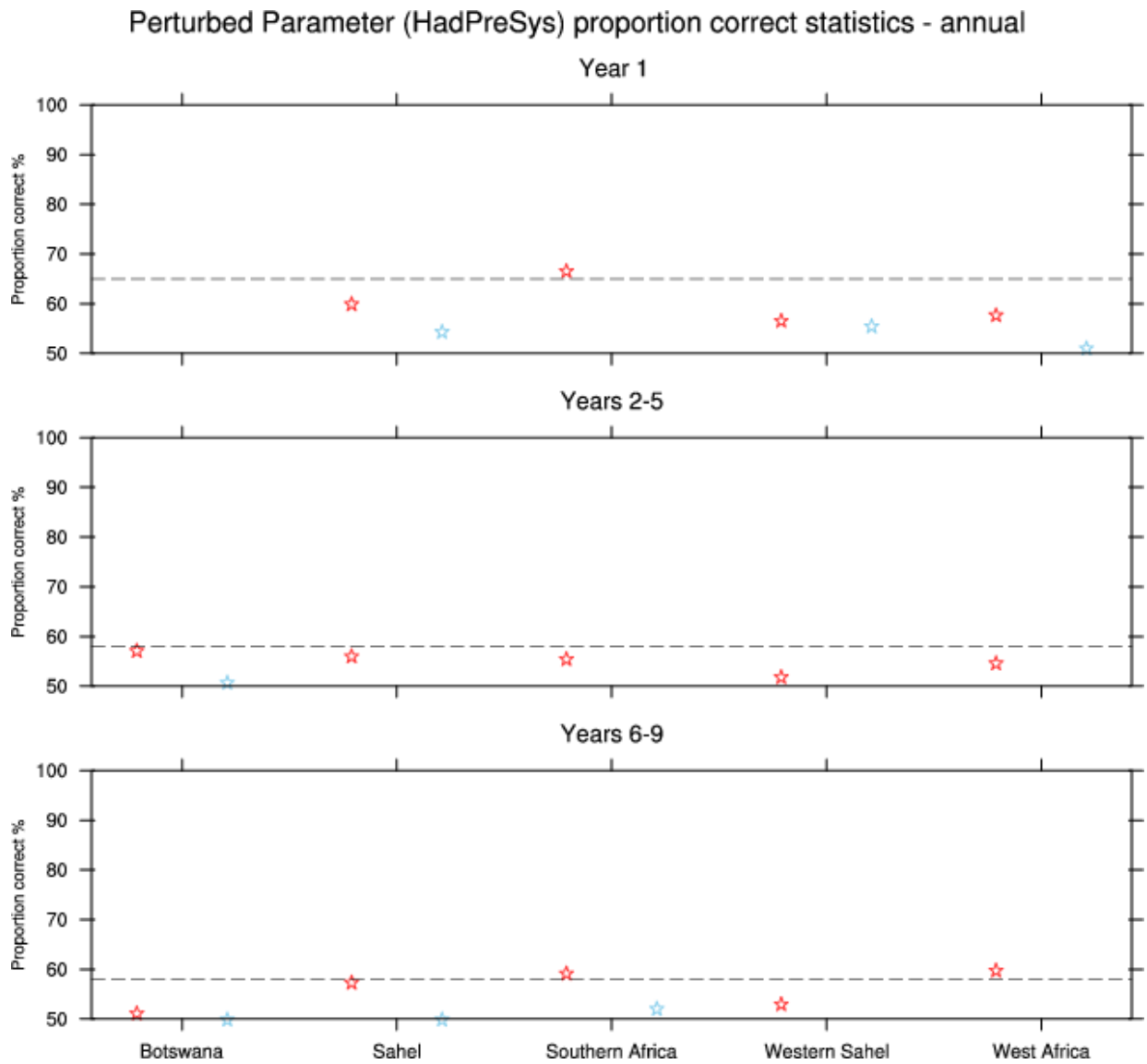


Figure 25. Same as Fig. 24, but for the ENSEMBLES perturbed-parameter decadal hindcast.

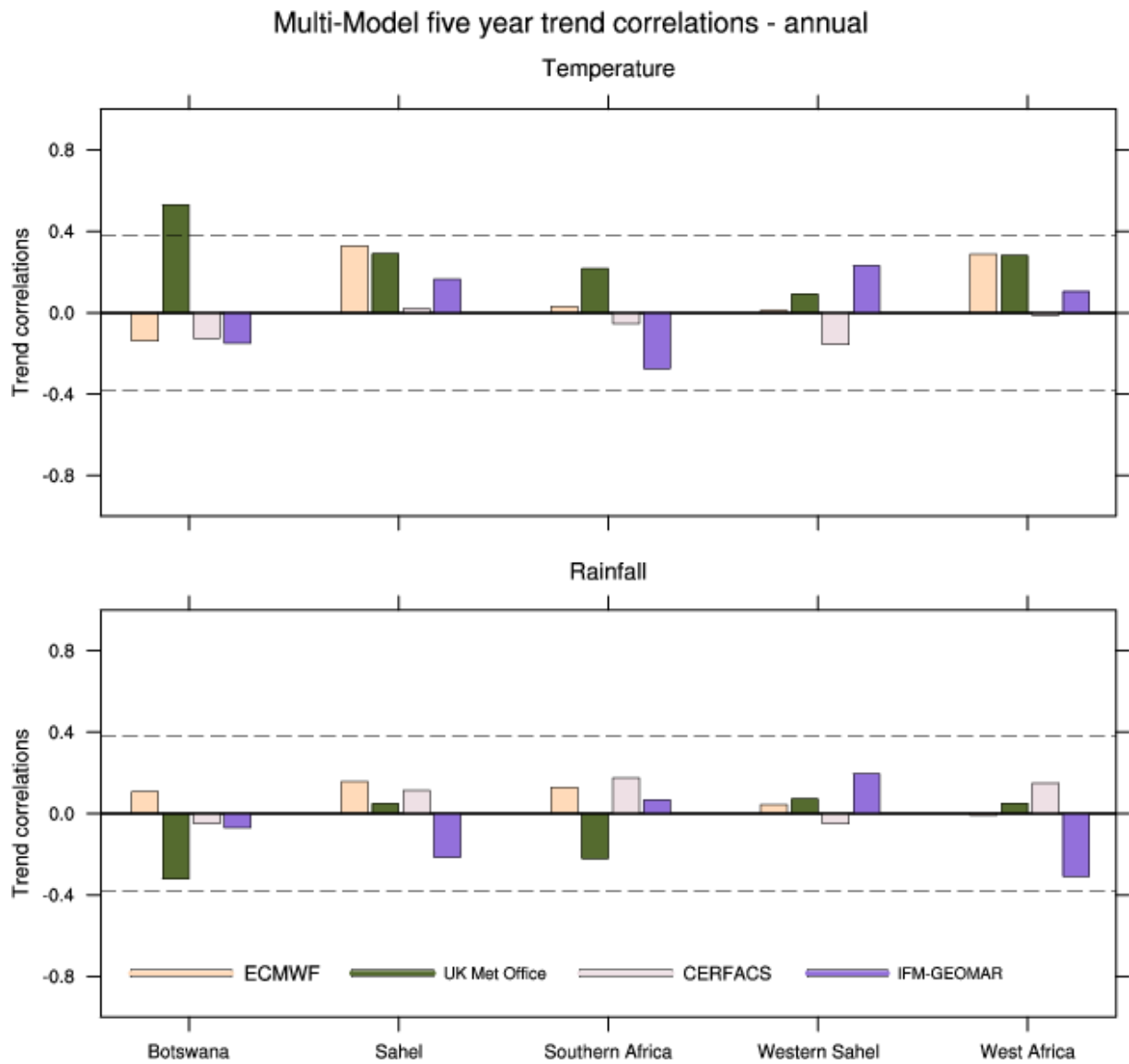


Figure 26. Correlations between simulated and observed five year T2m and precipitation trends, for ENSEMBLES decadal multi-model experiment, for the regions shown in Fig. 23. Note that the ocean is masked in all calculations. Dashed lines indicate 95% significance level.

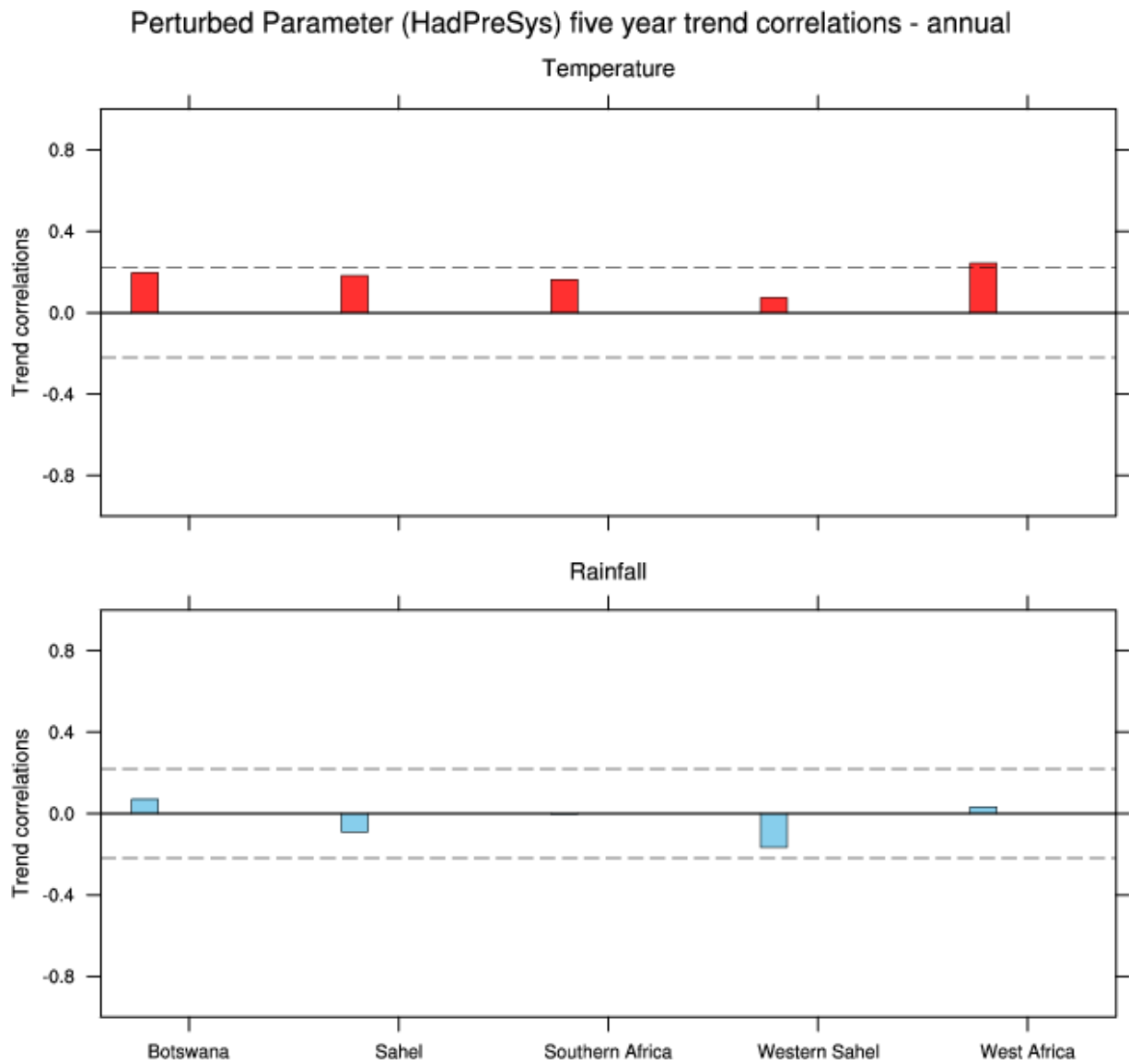


Figure 27. Same as Fig. 26, but for the ENSEMBLES perturbed-parameter decadal hindcast.